FACULTY OF MATHEMATICS, PHYSICS AND INFORMATICS
Comenius University
Bratislava

Local-limit disorder characteristics of niobium-based superconducting radio-frequency cavities (arXiv:2409.04203)

František Herman

Slovak Academic and Scientific Programme SAS PRO 2
APVV-23-0515, M. C. Grant Agreement No. 945478.

Motivation/Outline

- BCS + pair-breaking scatterings + pair-conserving scatterings = Dynes superconductor model.
- (Both) Scattering effects signatures in the superconducting optical conductivity response.
- (Both) Scattering effects in the superconducting surface impedance properties (in the local limit).

Pairing and Disorder

Superconductivity

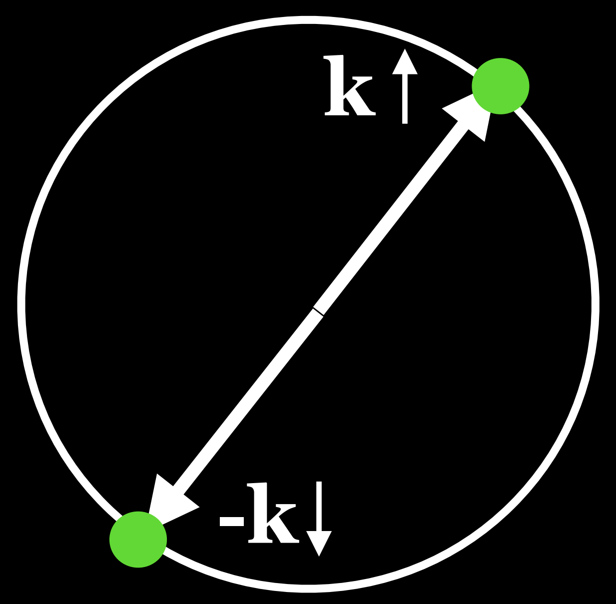

Δ

Pair-conserving, non-magnetic

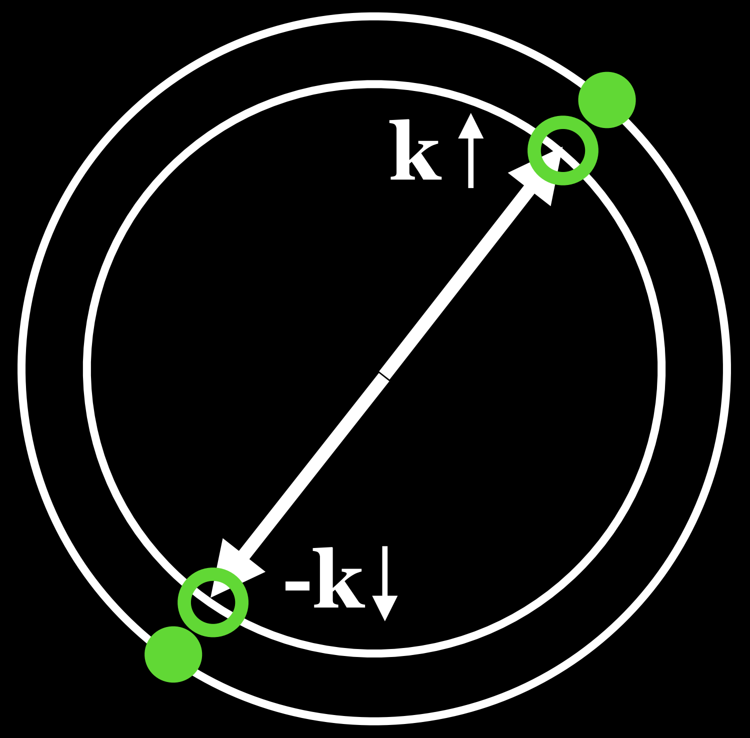

Γ_s

Pair-breaking, magnetic

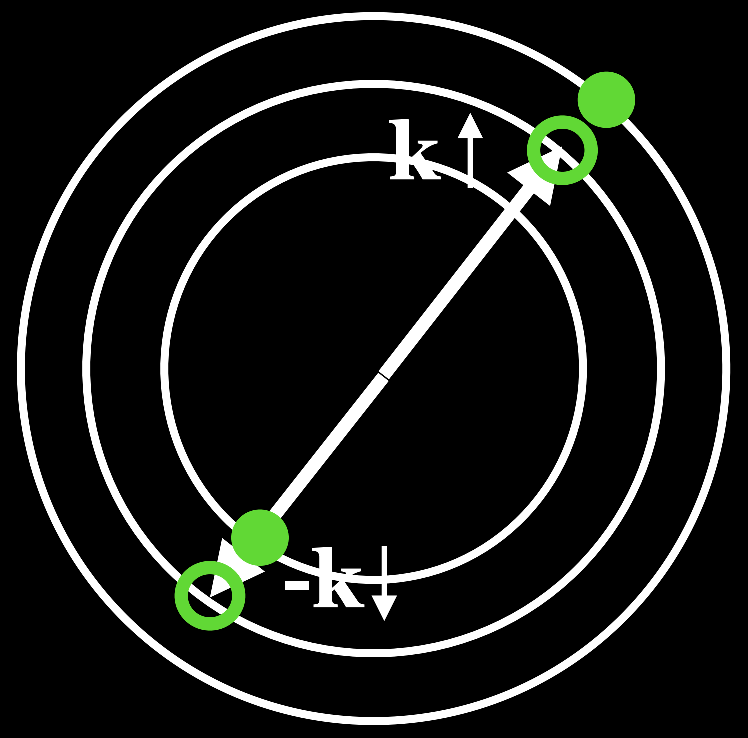

Γ

Dynes Formula

$$N(E) = \mathrm{Re}\left\{\frac{E + i\Gamma}{\sqrt{(E + i\Gamma)^2 - \Delta^2}}\right\}$$

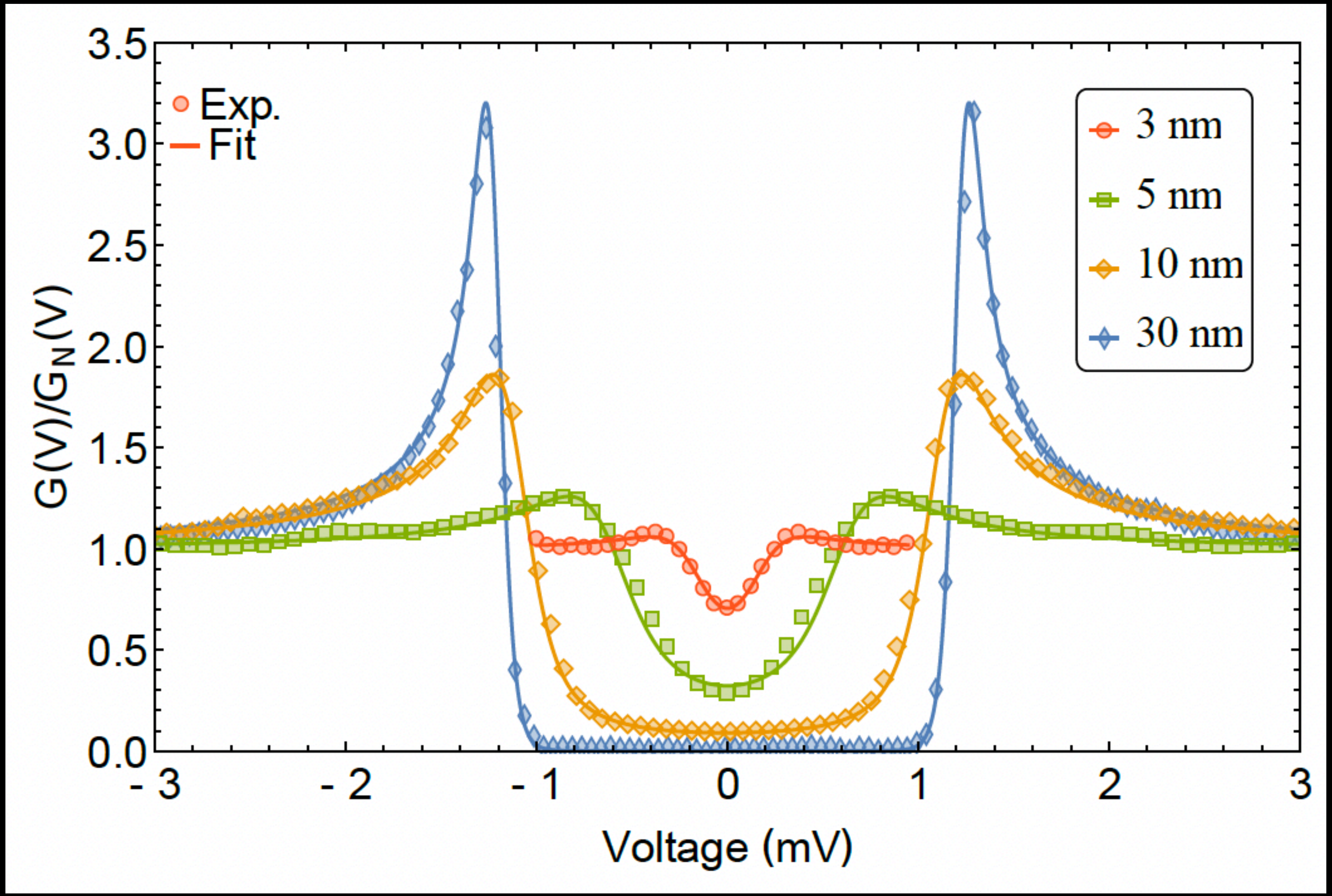

F. H., R. Hlubina, PRB **94**, 144508 (2016).

Dynes Superconductor

- Internally consistent extension of the BCS superconductor including pair-breaking and pair-conserving scattering processes in general case.
- Capable to describe electromagnetic and thermodynamic response.
- Applicable at low (density of states) and also higher (coherence peak) temperatures.
- Applicable at high disorder (MoC - superconductor-insulator transition) and low disorder (Nb-SRF motivated)
- Mathematical formulation using Green function method:

Dynes Superconductor

- Internally consistent extension of the BCS superconductor including pair-breaking and pair-conserving scattering processes in general case.
- Capable to describe electromagnetic and thermodynamic response.
- Applicable at low (density of states) and also higher (coherence peak) temperatures.
- Applicable at high disorder (MoC - superconductor-insulator transition) and low disorder (Nb-SRF motivated)
- Mathematical formulation using Green function method:

$$\hat{G}(\mathbf{k},\omega) = \frac{1}{2}\delta \ln\left[\varepsilon_{\mathbf{k}}^2 - \epsilon(\omega)^2\right],$$

$$\delta = \tau_0\partial_\omega - \tau_1\partial_\Delta - \tau_3\partial_{\varepsilon_{\mathbf{k}}},$$

$$\epsilon(\omega) = \sqrt{(\omega + i\Gamma)^2 - \Delta(T)^2} + i\Gamma_s.$$

5 energy scales.

Two-lifetime model for the cuprates revisited

Lucia Gelenekyová, František Herman, Hana Havranová, and Richard Hlubina
Department of Experimental Physics, Comenius University, Mlynská Dolina F2, 842 48 Bratislava, Slovakia
(Dated: February 3, 2026)

Several models of the strange-metal state of the cuprate superconductors postulate the existence of strong inelastic forward scattering of the electrons, but direct evidence of such scattering is missing. Here we show that angle-resolved photoemission spectroscopy (ARPES) provides a unique tool which can address this issue. We propose a two-lifetime phenomenological model of the superconducting state of the cuprates and we show that it explains several salient low-energy features of the measured ARPES spectra. The model enables discrimination between forward- and large-angle scattering and, in addition, gives access to the magnitude of the gap function away from the Fermi surface.

L. Gelenekyová et al., arXiv:2602.02097v1.

Dynes Superconductor - Optical Conductivity Response

$$\sigma(\omega) = \frac{i}{\omega + i0} K(\omega) \qquad K(\omega_m) = D_0 + \frac{e^2 v_F^2}{3} \int \frac{d^3\mathbf{k}}{(2\pi)^3} T \sum_{\omega_l} \mathrm{Tr}\left[\hat{G}(\mathbf{k}, \omega_l + \omega_m) \hat{G}(\mathbf{k}, \omega_l)\right]$$

Dirty limit, $\Gamma_s \gg \Delta, \Gamma$

$$\sigma'_{reg}(\omega) = \frac{\sigma_0}{\omega} \int_{-\infty}^{\infty} d\nu \left[f(\nu) - f(\nu + \omega)\right] \times \left[n'(\nu) n'(\nu + \omega) + p'(\nu) p'(\nu + \omega)\right]$$

$$n^2(\omega) - p^2(\omega) = 1$$

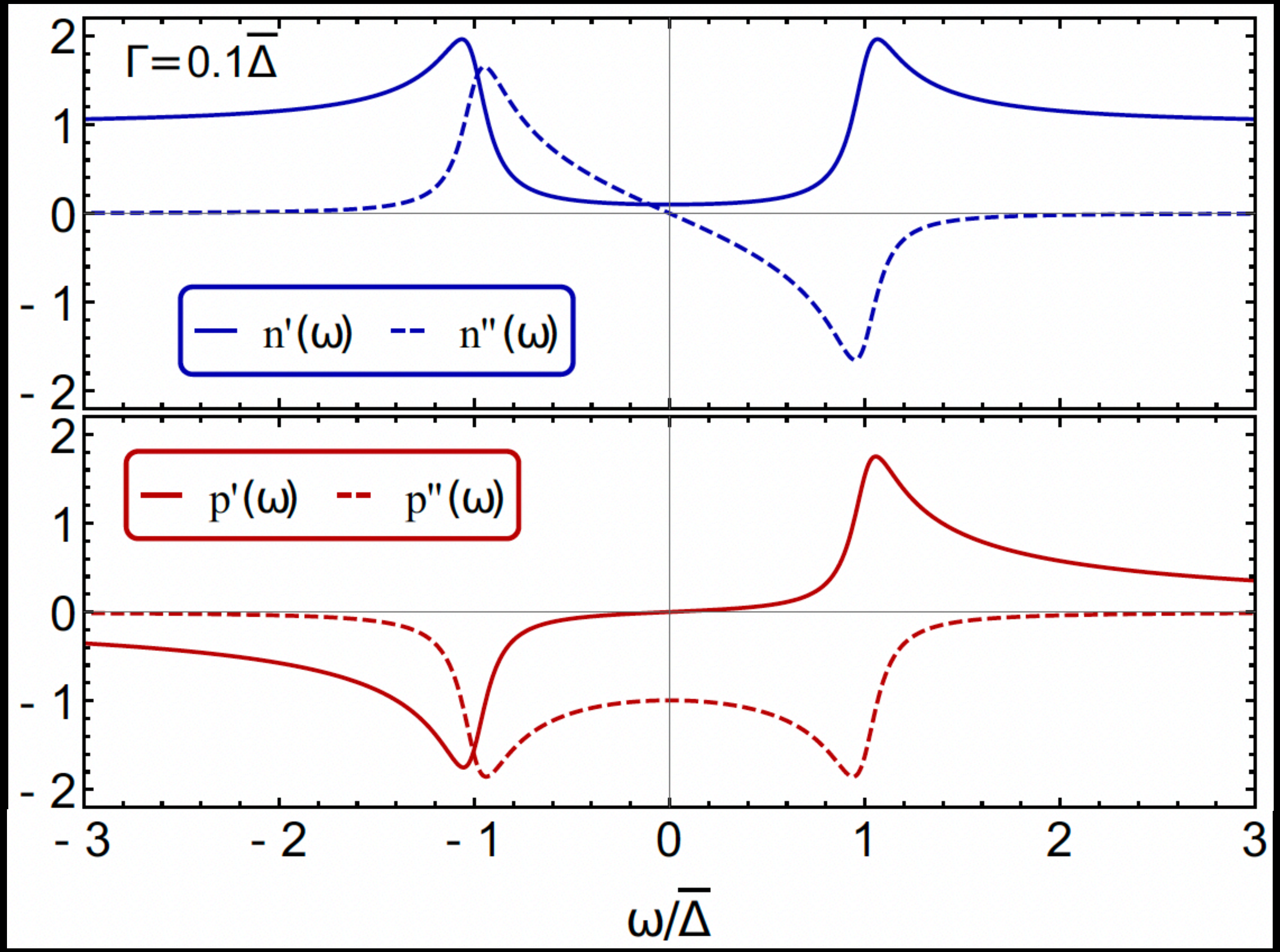

Dynes Superconductor - Optical Conductivity Response

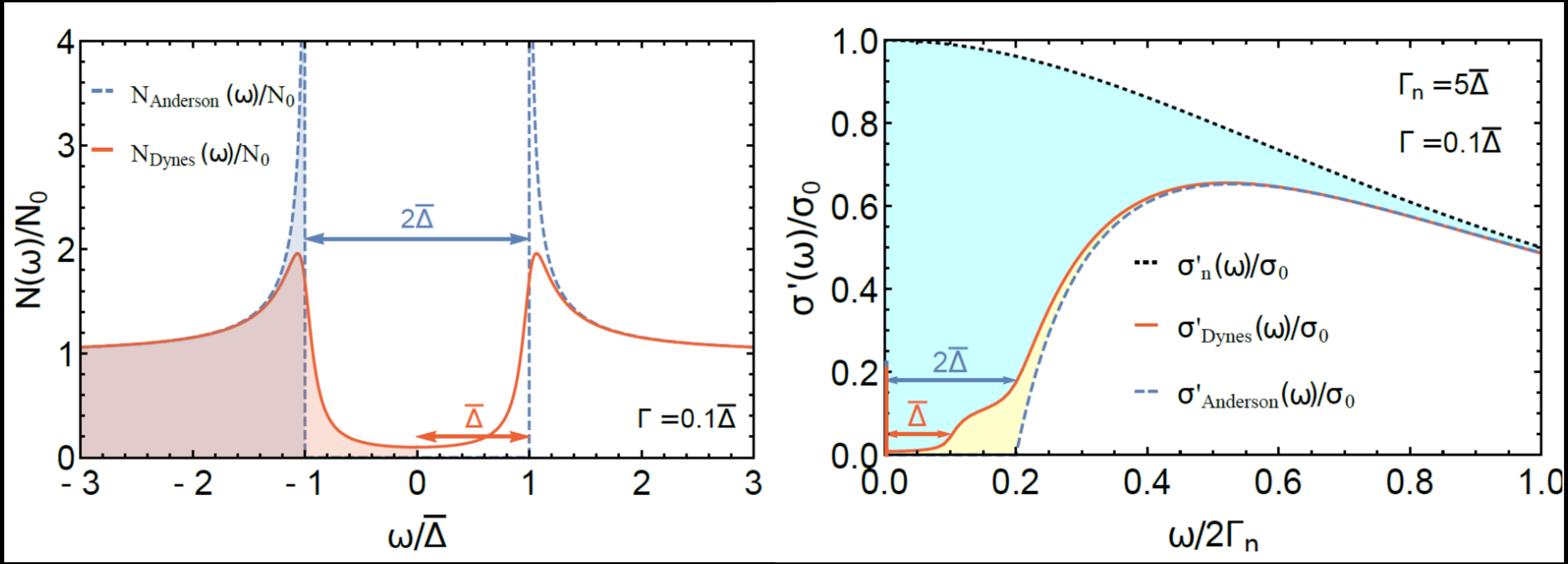

F. H. and R. Hlubina, Phys. Rev. B **104**, 094519 (2021)

Dynes Superconductor - Optical Conductivity Response

F. Bolle *et al.*, arXiv:2602.15003v1.

Dynes Superconductor

Electromagnetic properties and (real part of the) optical conductivity

- *Implications towards the superconducting cavities: Coherence peak*

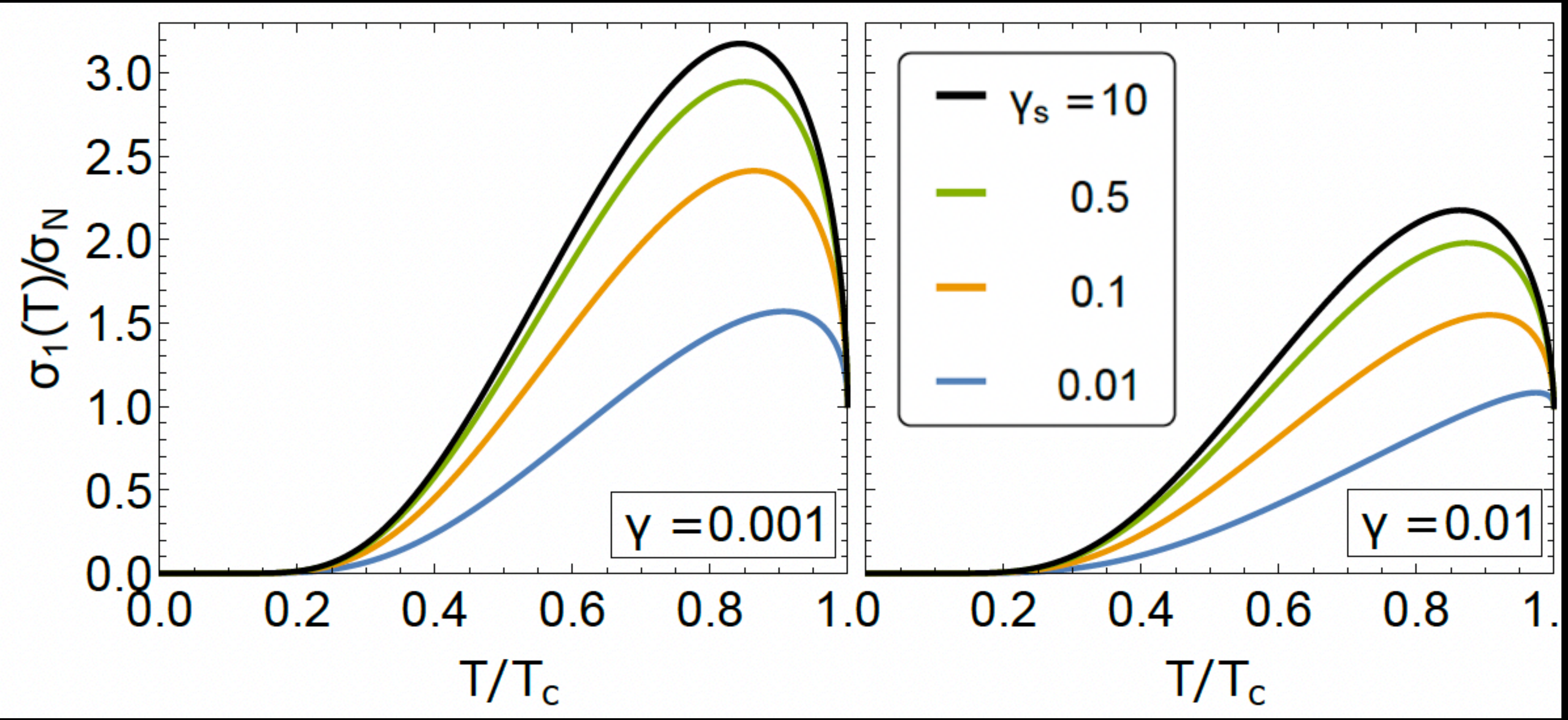

F. H. and R. Hlubina, Phys. Rev. B **104**, 094519 (2021)

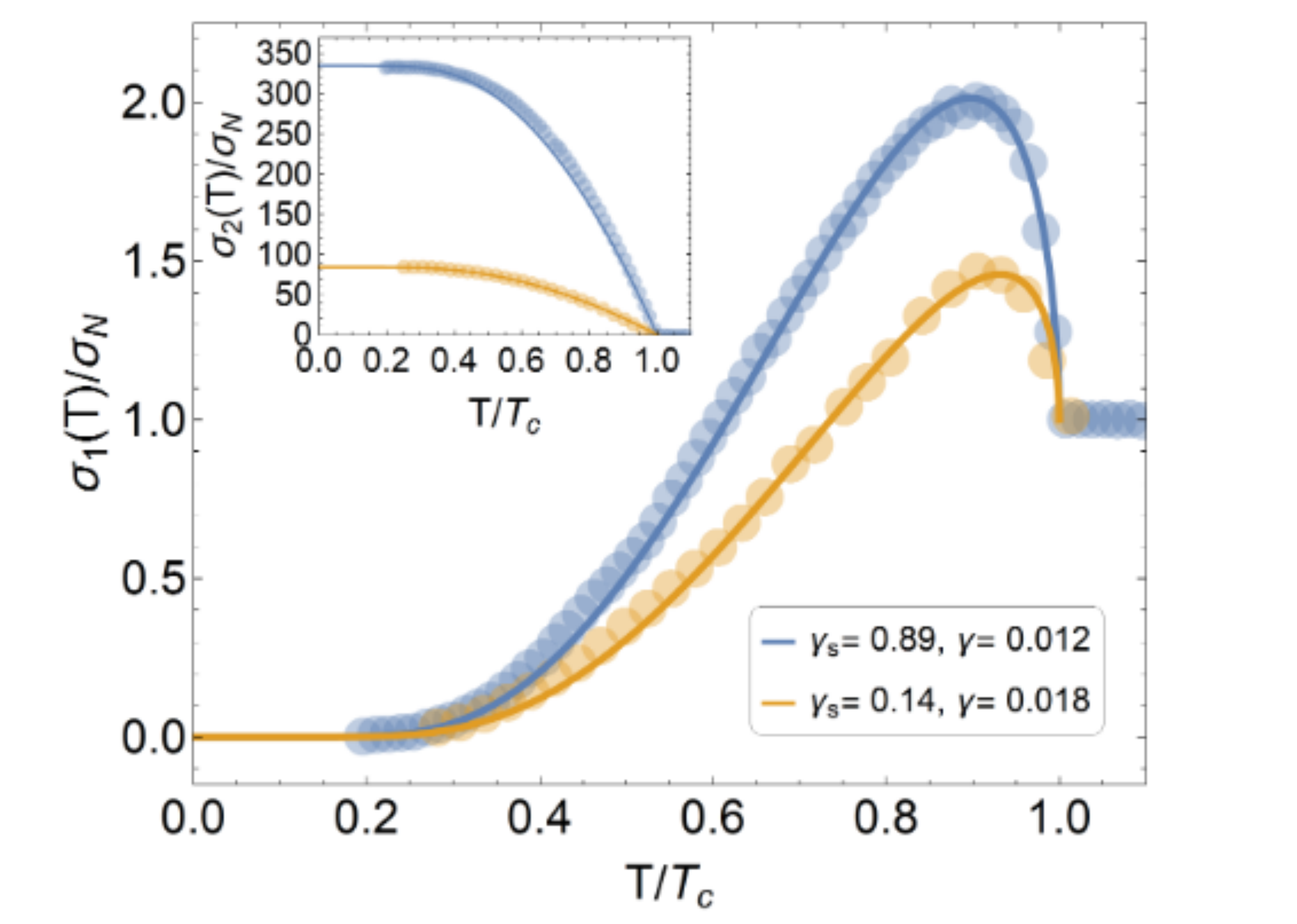

FIG. 9. Real and imaginary parts of the conductivities of the two samples from Fig. 4 in [13] (symbols), together with their fits by the theory of Dynes superconductors with the strong-coupling corrections described for both samples by $x = 1.145$ (lines).

D. Bafia et al., ArXiv:2106.10601 (2021)

Dynes Superconductor

Electromagnetic properties and (real part of the) optical conductivity

- *Implications towards the superconducting cavities: Coherence peak*

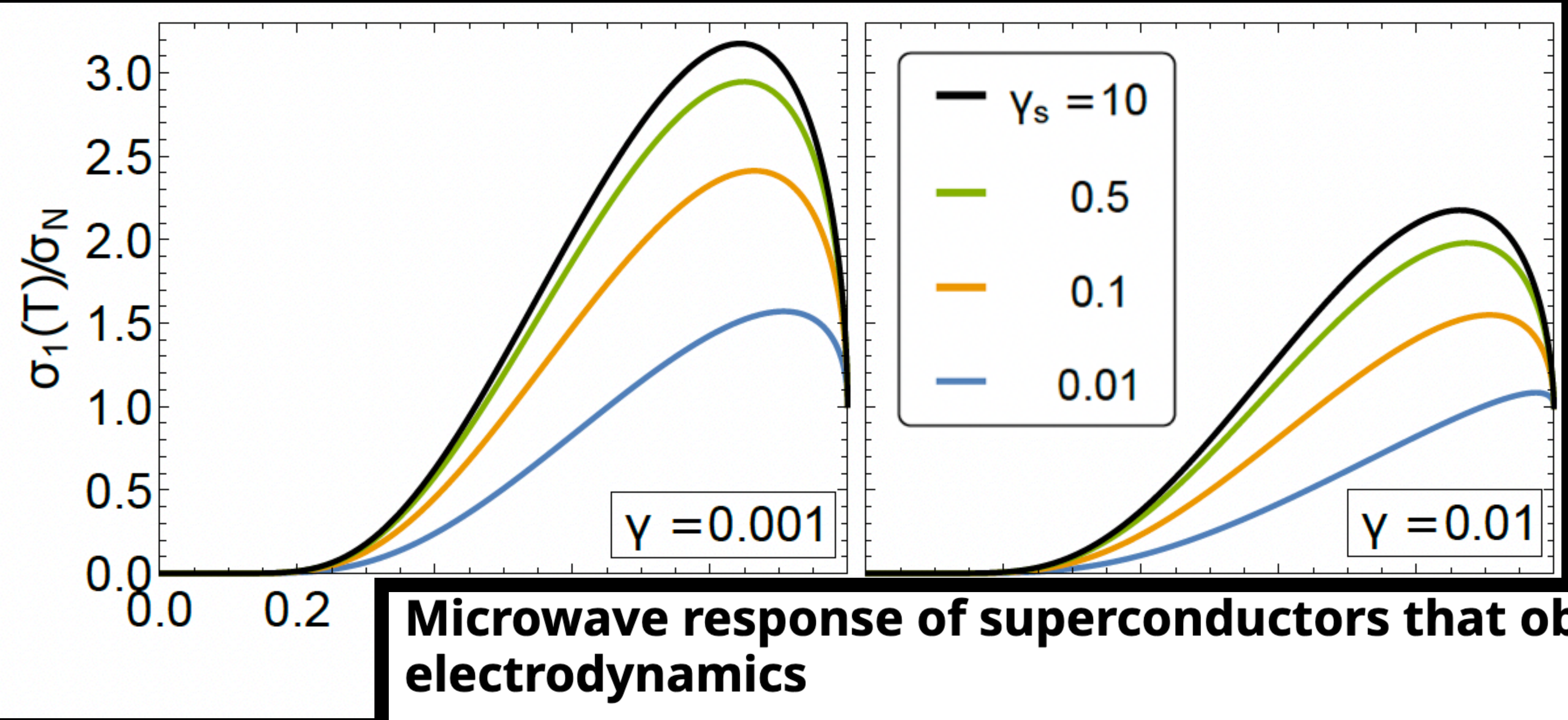

F. H. and R. Hlubir

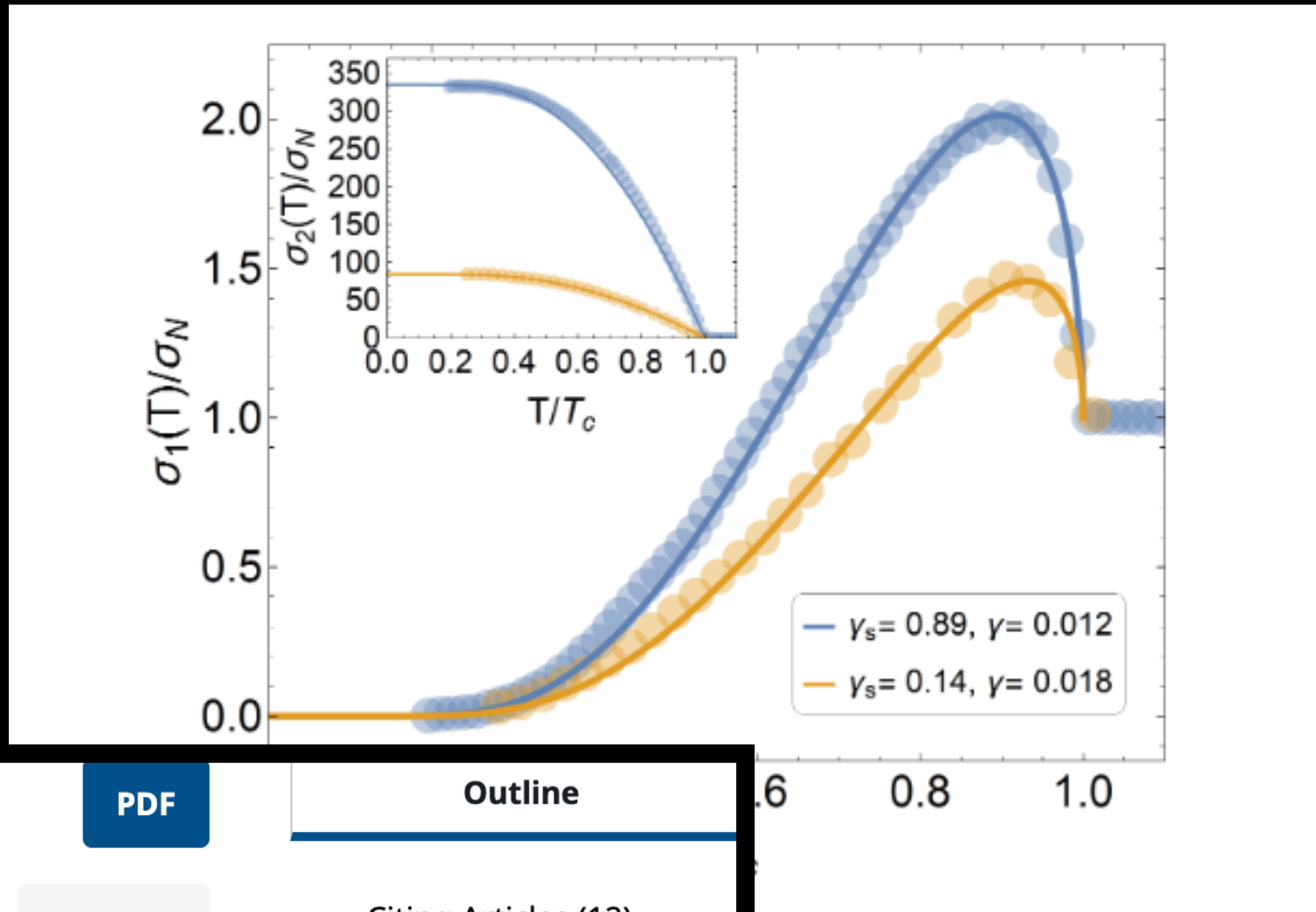

f the conductivities of the
nbols), together with their
nductors with the strong-
oth samples by $x = 1.145$

1 (2021)

Microwave response of superconductors that obey local electrodynamics

PDF

Share

František Herman and Richard Hlubina

Show more

Phys. Rev. B **104**, 094519 – **Published 21 September, 2021**

DOI: https://doi.org/10.1103/PhysRevB.104.094519

Export Citation

Outline

Citing Articles (12)

Abstract

Article Text

Supplemental Material

References

FACULTY OF MATHEMATICS, PHYSICS AND INFORMATICS
Comenius University
Bratislava

Physical Review Applied

Local-limit disorder characteristics of niobium-based superconducting radio-frequency cavities

Anastasiya Lebedeva*, Matúš Hladký*, Marcel Polák, and František Herman†

Show more

herman2@uniba.sk

Phys. Rev. Applied **24**, 044007 – **Published 2 October, 2025**

arXiv:2409.04203

DOI: https://doi.org/10.1103/5hp2-3x8n

Anastasiya Lebedeva

Matúš Hladký

Marcel Polák

Frequency shift & Quality factor

Slovak Academic and Scientific Programme | SASPRO 2

APVV-23-0515, M. C. Grant Agreement No. 945478.

Fundamental Physics

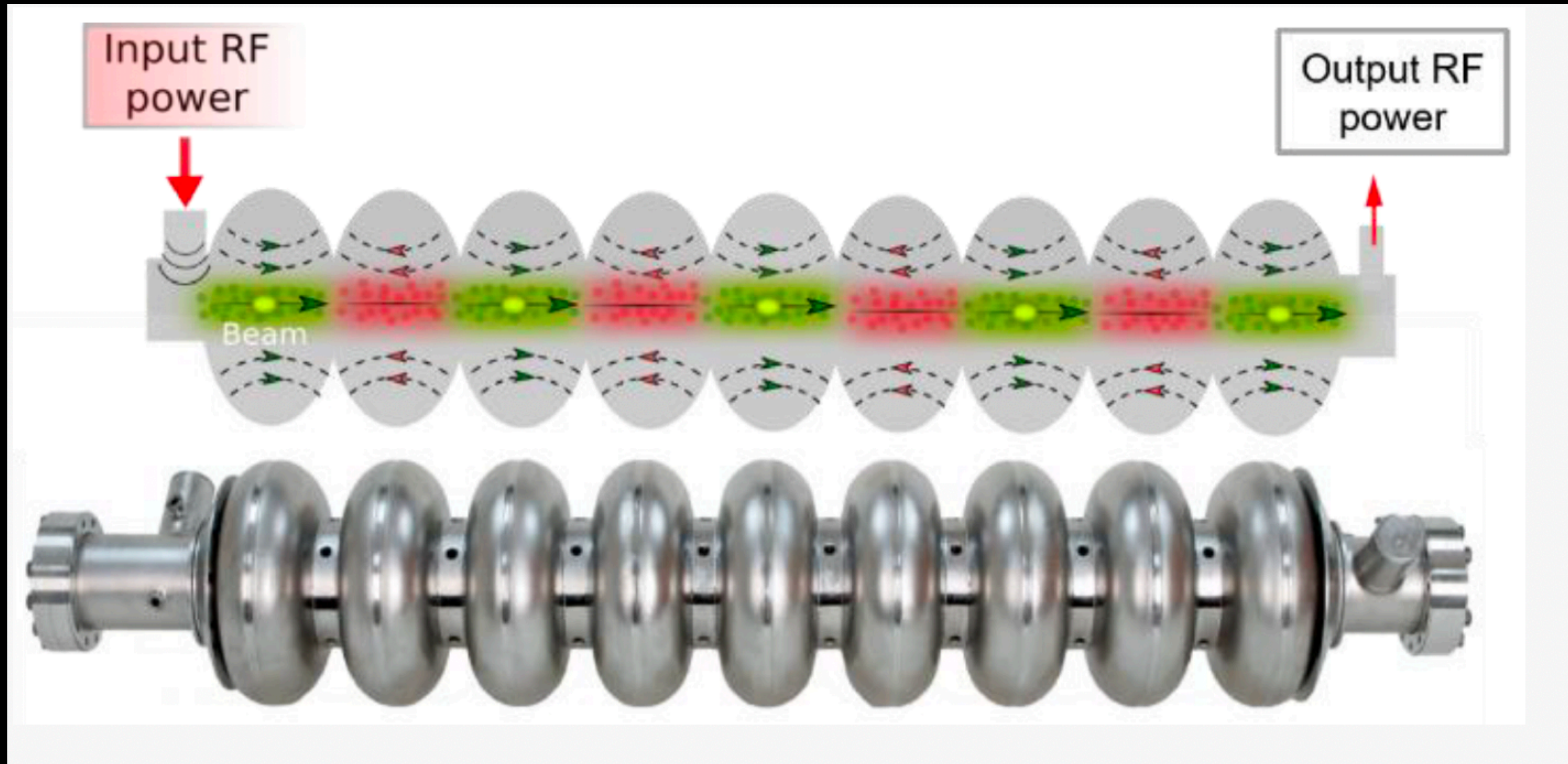

[O. Hryhorenko et al., J. Manuf. Mater. Process. 2023, 7(2), 62]

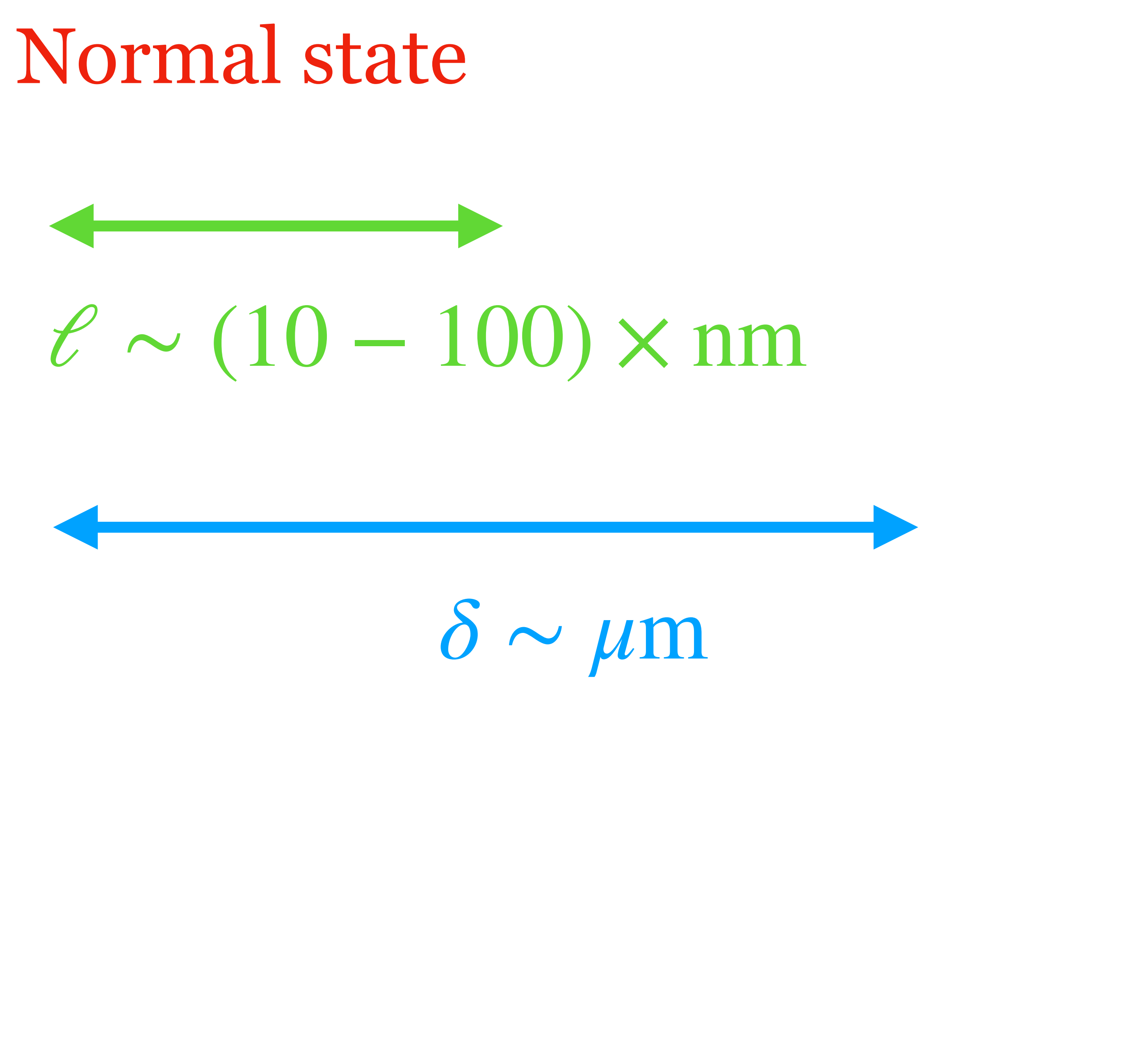

Fundamental Physics

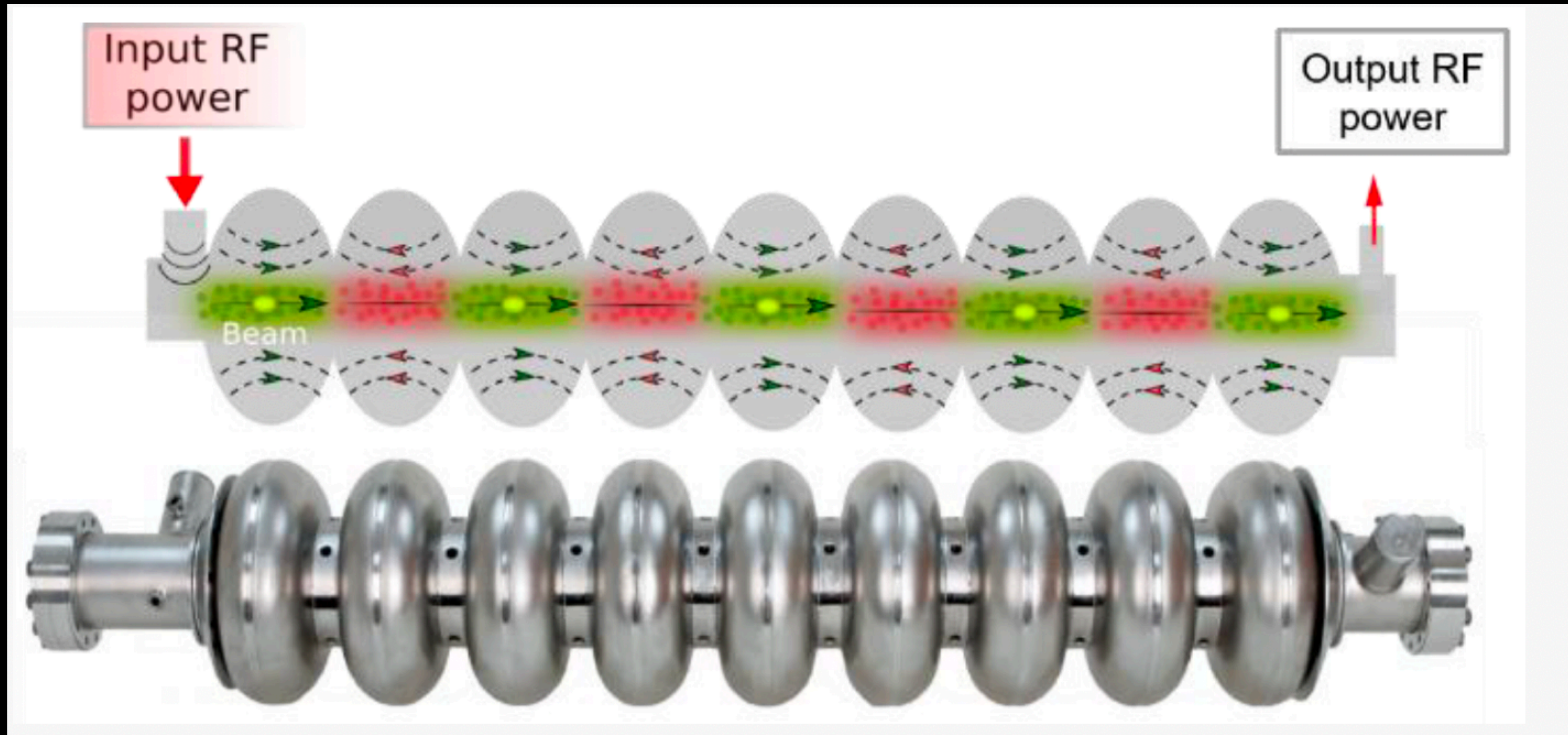

[O. Hryhorenko et al., J. Manuf. Mater. Process. 2023, 7(2), 62]

Superconducting state $T \sim 0\text{K}$

$\ell \sim (10-100) \times \text{nm}$

$\lambda_L(0) \sim 10 \times \text{nm}$

$\xi \sim 10 \times \text{nm}$

Normal state

$\ell \sim (10-100) \times \text{nm}$

$\delta \sim \mu\text{m}$

Fundamental Physics

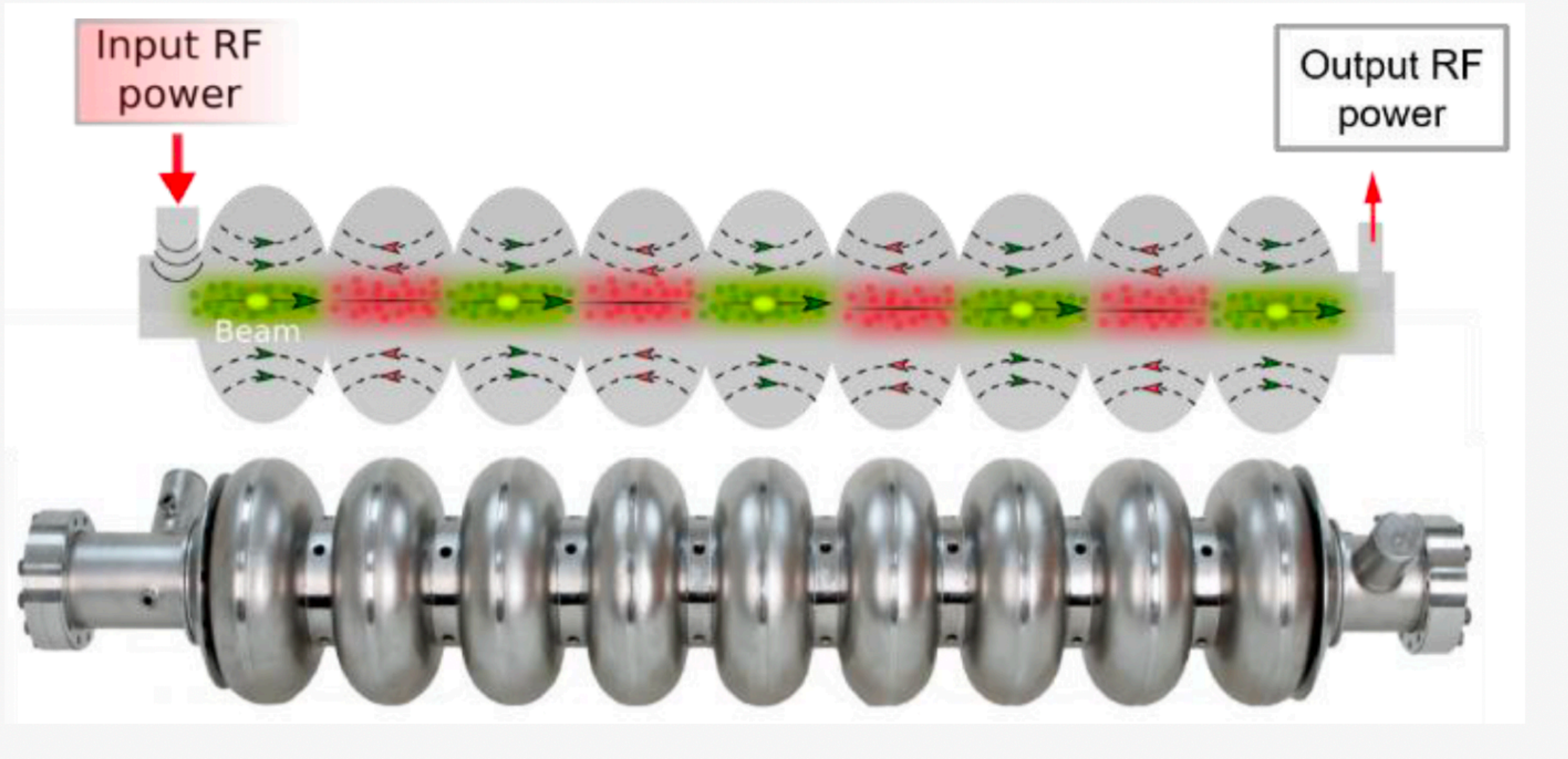

[O. Hryhorenko et al., J. Manuf. Mater. Process. 2023, 7(2), 62]

Superconducting state $T \sim 0\mathrm{K}$

$\ell \sim (10-100) \times \mathrm{nm}$

$\lambda_L(0) \sim 10 \times \mathrm{nm}$

$\xi \sim 10 \times \mathrm{nm}$

Superconducting state $T \to T_c$

$\ell \sim (10-100) \times \mathrm{nm}$

$\lambda_L(T) \to \infty$

$\xi \sim 10 \times \mathrm{nm}$

Normal state

$\ell \sim (10-100) \times \mathrm{nm}$

$\delta \sim \mu\mathrm{m}$

Surface Impedance (Z) *& microwave conductivity* (σ)

$$\frac{Z_s}{Z_n} = \frac{R_s + iX_s}{R_n + iX_n} = \left(\frac{\sigma_1 - i\sigma_2}{\sigma_n}\right)^k$$

- R - surface resistance, X - surface reactance

Frequency shift $\delta f(T)$

$$\frac{\delta f(T)}{\tilde{f}} = 1 - \frac{X_s(T)}{X_n}$$

Frequency shift $\delta f(T)$

$$\frac{\delta f(T)}{\tilde{f}} = 1 - \frac{X_s(T)}{X_n} \qquad \tilde{f} \equiv \frac{fX_n}{2G} \sim (1-10) \times \mathrm{kHz}$$

Frequency shift $\delta f(T)$

$$\frac{\delta f(T)}{\tilde{f}} = 1 - \frac{X_s(T)}{X_n}$$

$$\tilde{f} \equiv \frac{f X_n}{2G} \sim (1 - 10) \times \mathrm{kHz}$$

$$\frac{\delta f(0)}{\tilde{f}} = 1 - \frac{2\lambda_L(0)}{\delta}$$

Nb Cavities at DESY, Hamburg

$$\frac{\delta f(T)}{\tilde{f}} = 1 - \frac{X_s(T)}{X_n} \qquad \tilde{f} \equiv \frac{fX_n}{2G} \sim (1 - 10) \times \mathrm{kHz} \qquad \frac{\delta f(0)}{\tilde{f}} = 1 - \frac{2\lambda_L(0)}{\delta}$$

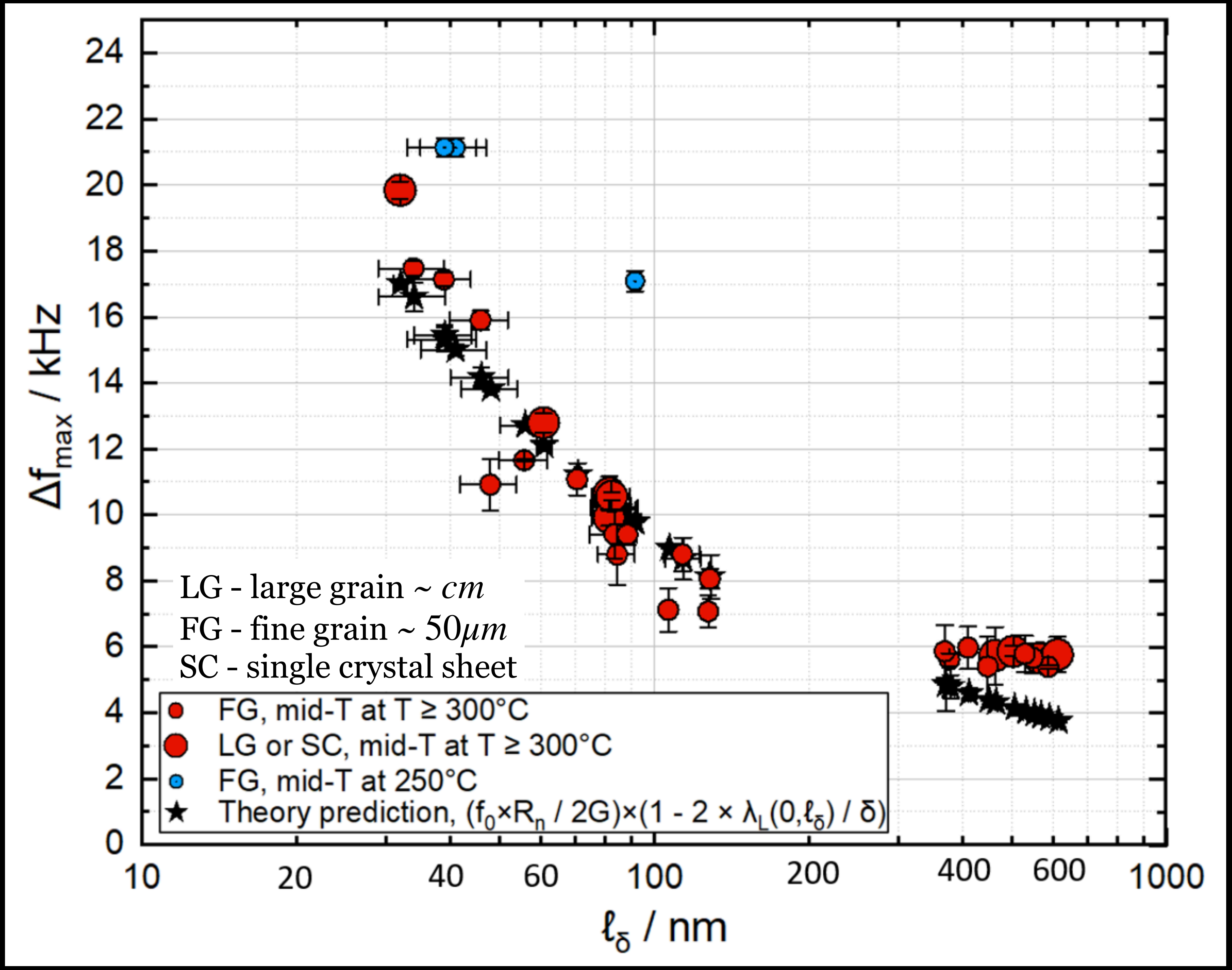

With the acknowledgment and consent of Marc Wenskat and Rezvan Ghanbari.

Nb Cavities at DESY, Hamburg

$$\frac{\delta f(T)}{\tilde{f}} = 1 - \frac{X_s(T)}{X_n} \qquad \tilde{f} \equiv \frac{fX_n}{2G} \sim (1-10)\times \mathrm{kHz} \qquad \frac{\delta f(0)}{\tilde{f}} = 1 - \frac{2\lambda_L(0)}{\delta}$$

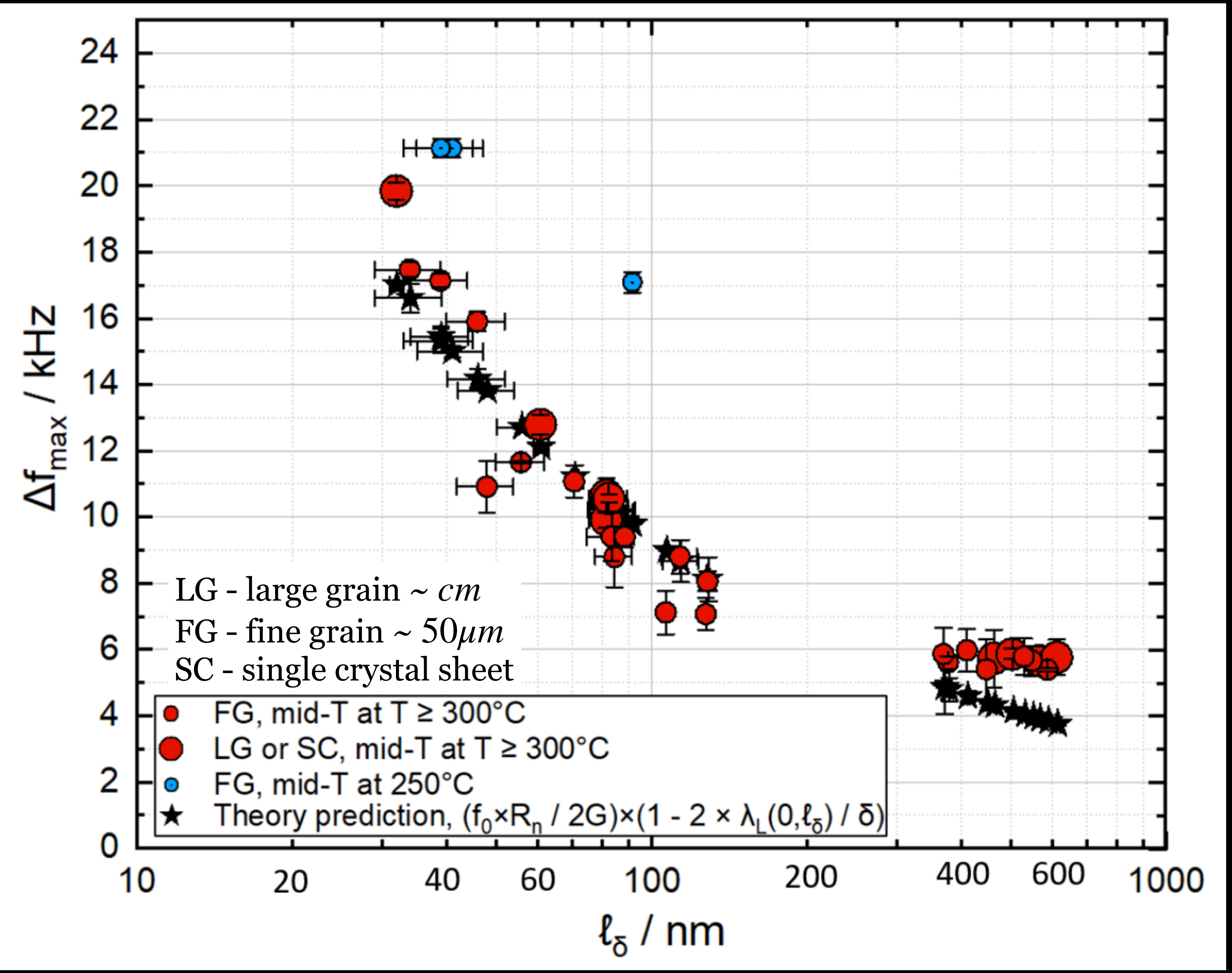

$$\Delta T_c[\mathrm{K}] \equiv T_{c0} - T_c,$$
$$= 0.93[\mathrm{K/at.\%}] \times c\,[\mathrm{at.\%}]$$

W. DeSorbo, Effect of Dissolved Gases on Some Superconducting Properties of Niobium, PHYS. REV., **132**, 1 (1963).

$$c \approx 0.1\ \mathrm{at.\%}$$

$$k_B \Delta T_c = (\pi/4)\Gamma$$
$$= J[\mathrm{eV}]c[\mathrm{at.\%}]/100$$

$$\Gamma \approx 0.01\ \mathrm{meV}$$
$$J \approx 10\ \mathrm{meV}$$

With the acknowledgment and consent of Marc Wenskat and Rezvan Ghanbari.

Frequency shift $\delta f(T)$

$$\frac{\delta f(T)}{\tilde{f}} = 1 - \frac{X_s(T)}{X_n} \qquad \tilde{f} \equiv \frac{f X_n}{2G} \sim (1-10) \times \mathrm{kHz} \qquad \frac{\delta f(0)}{\tilde{f}} = 1 - \frac{2\lambda_L(0)}{\delta}$$

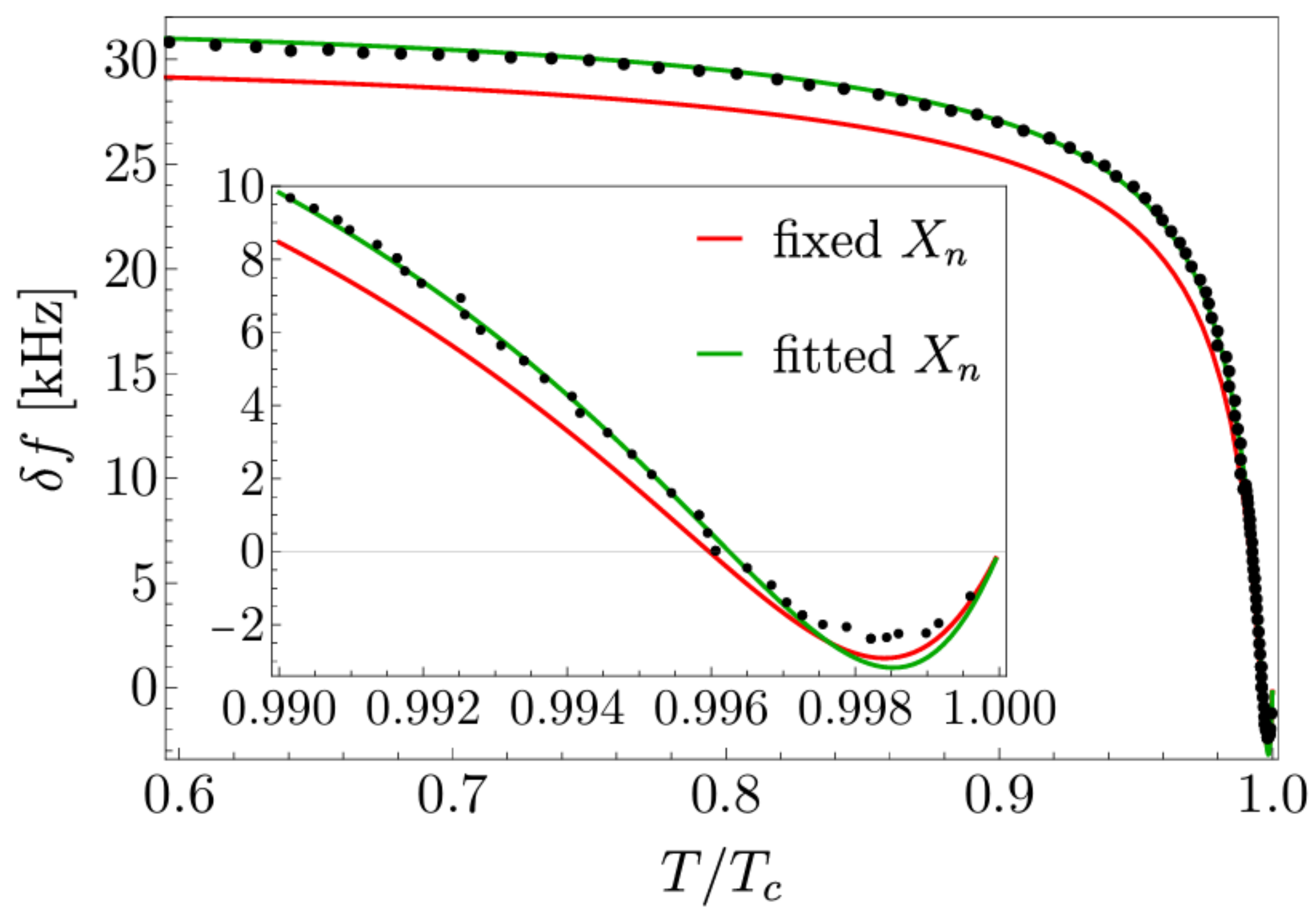

FIG. 7. Considered parameters: resonant frequency $f = 2.6\,\mathrm{GHz}$, $\Delta_0 = 1.55\,\mathrm{meV}$ [1], pair-conserving scattering rate corresponding to fixed $X_n = 7.1\,\mathrm{m}\Omega$ (fitted $X_n = 7.5\,\mathrm{m}\Omega$) is $\gamma_s = 0.52$ ($\gamma_s = 0.58$), and resulting $\ell = 121\,\mathrm{nm}$ ($\ell = 108\,\mathrm{nm}$).

Data from: M. Zarea, H. Ueki, and J. A. Sauls, Frontiers in Superconducting Materials, 3: 1-7.

Frequency shift $\delta f(T)$

$$\frac{\delta f(T)}{\tilde{f}} = 1 - \frac{X_s(T)}{X_n} \qquad \tilde{f} \equiv \frac{fX_n}{2G} \sim (1-10)\times \mathrm{kHz} \qquad \frac{\delta f(0)}{\tilde{f}} = 1 - \frac{2\lambda_L(0)}{\delta}$$

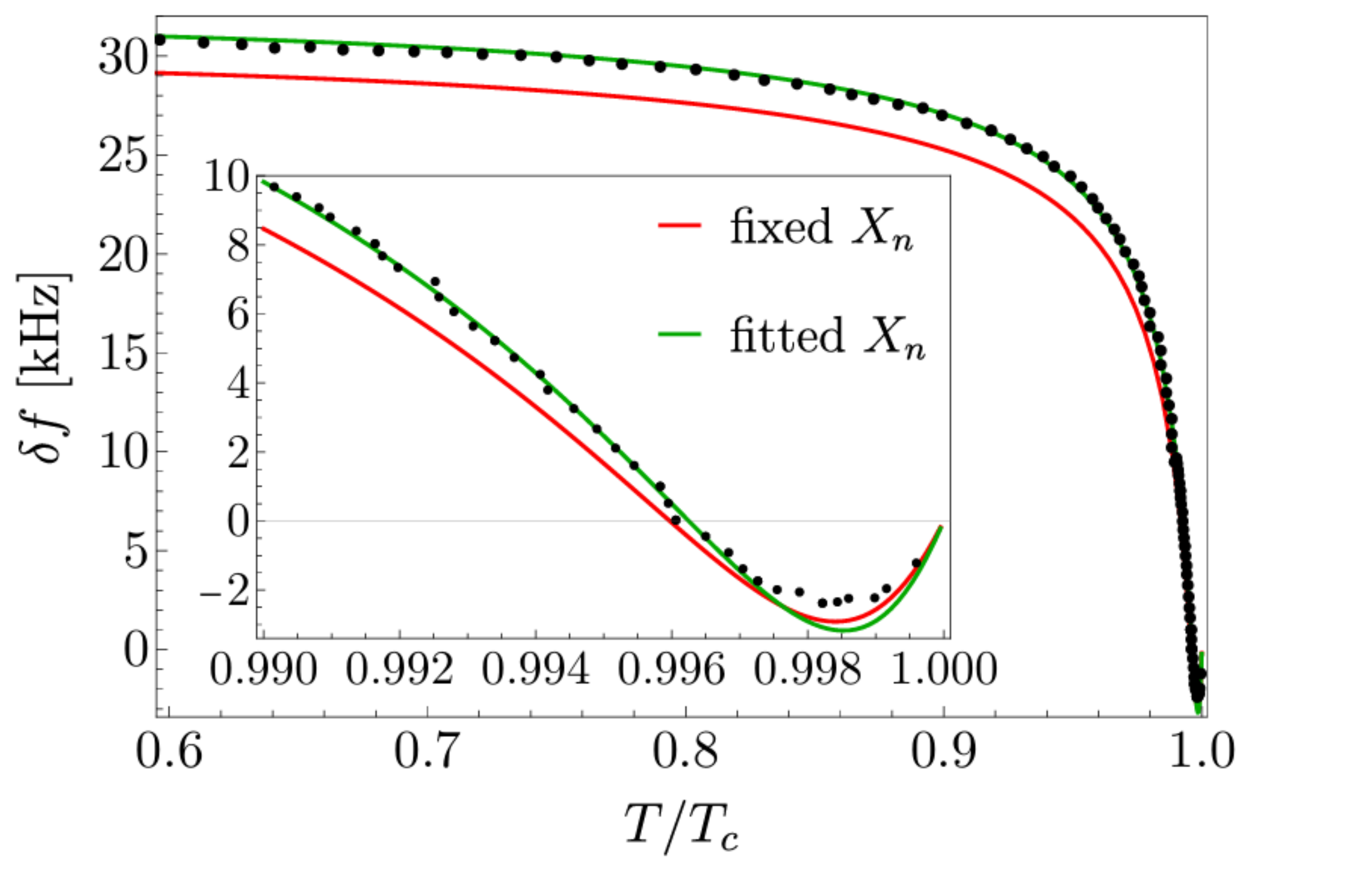

FIG. 7. Considered parameters: resonant frequency $f = 2.6\,\mathrm{GHz}$, $\Delta_0 = 1.55\,\mathrm{meV}$ [1], pair-conserving scattering rate corresponding to fixed $X_n = 7.1\,\mathrm{m}\Omega$ (fitted $X_n = 7.5\,\mathrm{m}\Omega$) is $\gamma_s = 0.52$ ($\gamma_s = 0.58$), and resulting $\ell = 121\,\mathrm{nm}$ ($\ell = 108\,\mathrm{nm}$).

Data from: M. Zarea, H. Ueki, and J. A. Sauls, Frontiers in Superconducting Materials, 3: 1-7.

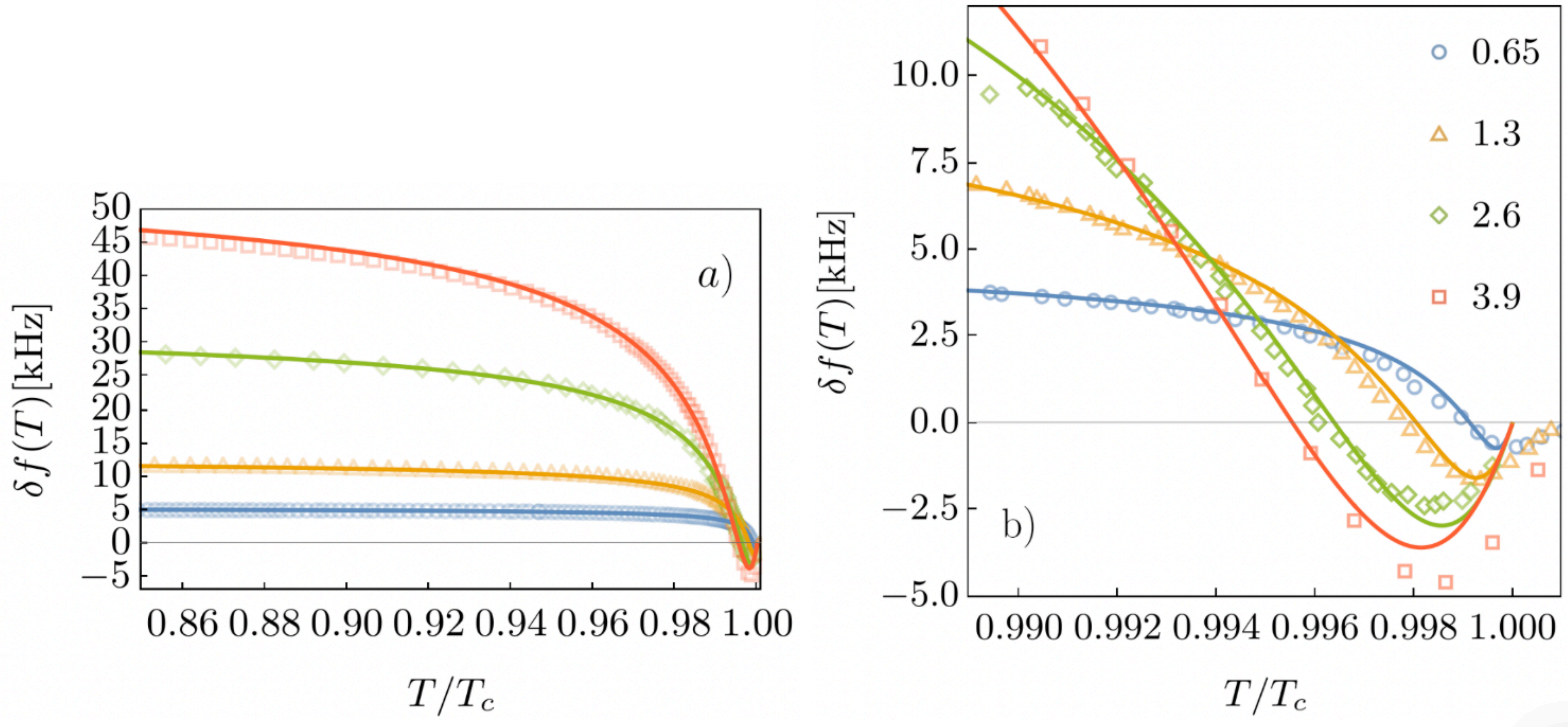

Data from: H. Ueki, M. Zarea, J. A. Sauls, Prog. Theor. Expt. Phys. 2025, **5**, 053102 (2025)

f [GHz]	R_n[mΩ]	T_c [K]	Γ [meV]	Γ_n [meV]	Δ_0[meV]
0.65	4.451	8.959	0.044	1.330	1.546
1.3	5.642	8.875	0.054	1.068	1.536
2.6	7.506	9.061	0.032	0.945	1.558
3.9	9.377	9.135	0.024	0.983	1.567

Various regimes, Experiment & Theory

D. Bafia et al., arXiv:2103.10601v2

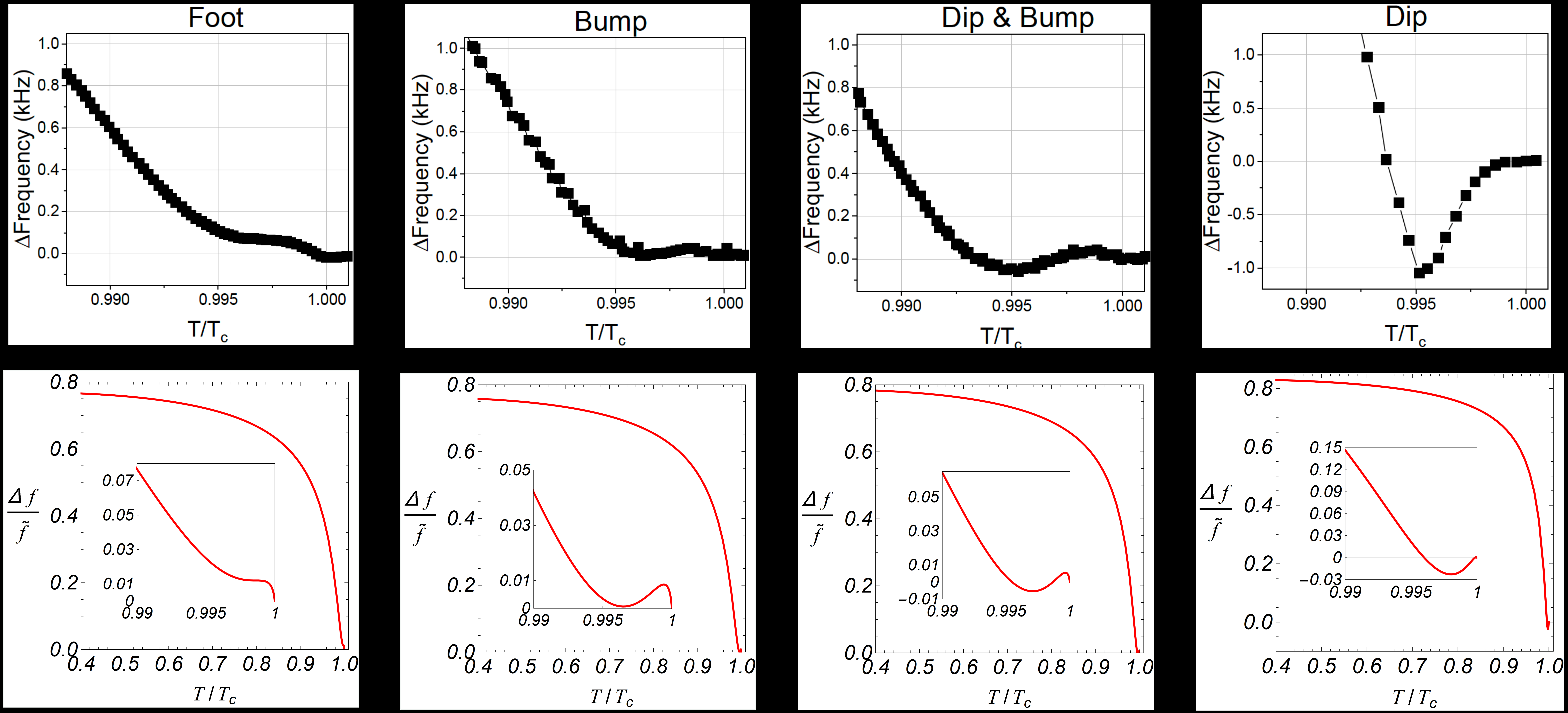

Moderately clean regime: $\hbar\omega < \Gamma \ll \Gamma_s \lesssim \Delta_0$

$$\delta f'(\Theta) \equiv \left.\frac{\partial \delta f(\Theta)}{\partial \Theta}\right|_{\Theta=0} \quad \text{where:} \quad \Theta = 1 - T/T_c$$

Moderately clean regime: $\hbar\omega < \Gamma \ll \Gamma_s \lesssim \Delta_0$

$$\delta f'(\Theta) \equiv \left.\frac{\partial \delta f(\Theta)}{\partial \Theta}\right|_{\Theta=0} \quad \text{where:} \quad \Theta = 1 - T/T_c$$

$$\sigma_s'(T)/\sigma_0 = 1 + f_1(\Gamma,\Gamma_s)\Theta, \quad \sigma_s''(T)/\sigma_0 = f_2(\Gamma,\Gamma_s,\omega)\Theta\,.$$

$$\delta f(T \to T_c)/\tilde{f} = \left(f_1 - f_2\right)\Theta/2$$

Moderately clean regime: $\hbar\omega < \Gamma \ll \Gamma_s \lesssim \Delta_0$

$$\delta f'(\Theta) \equiv \left.\frac{\partial \delta f(\Theta)}{\partial \Theta}\right|_{\Theta=0} \quad \text{where:} \quad \Theta = 1 - T/T_c$$

$$\sigma_s'(T)/\sigma_0 = 1 + f_1(\Gamma, \Gamma_s)\Theta, \quad \sigma_s''(T)/\sigma_0 = f_2(\Gamma, \Gamma_s, \omega)\Theta\,.$$

$$\delta f(T \to T_c)/\tilde{f} = \left(f_1 - f_2\right)\Theta/2$$

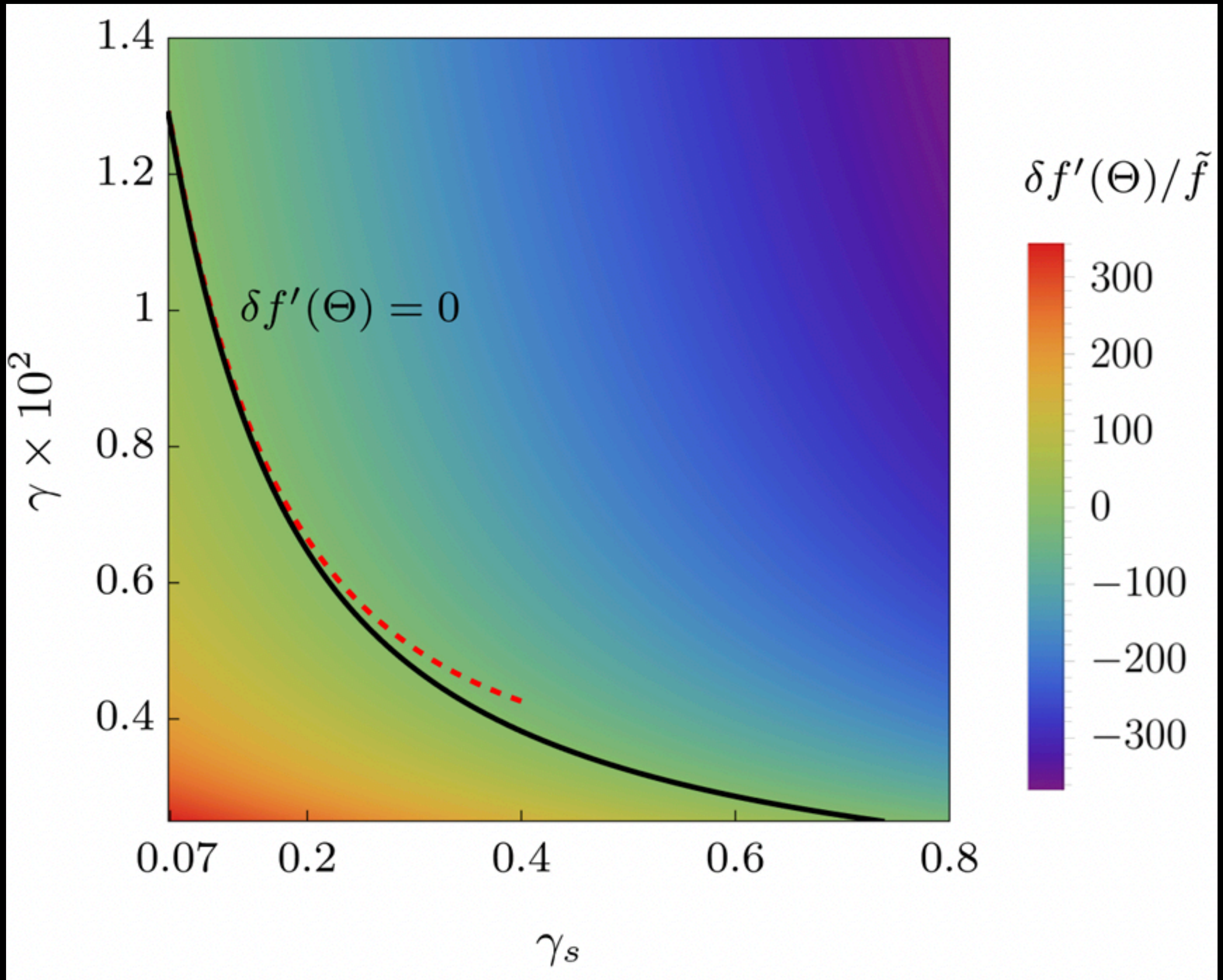

1) $\Gamma \ll T_c \sim \Delta_{00}$

$$f_1(\Gamma, \Gamma_s) \sim \frac{\Delta_{00}}{\Gamma}$$

$$f_2(\Gamma, \Gamma_s, \omega) \sim \left(\frac{\delta}{\lambda_L(0)}\right)^2$$

- Both signs are possible.

2) $\Gamma \gg T_c$ with arbitrary Γ_s

$$f_1 \sim -\left(\frac{\Delta_0}{\Gamma}\right)^2 < 0$$

- Pure dip.

Quality $Q_s = G/R_s$ in local limit

$$\frac{Q_s}{Q_n} = \left(\frac{|\sigma_s|}{|\sigma_n|}\right)^{1/2} \frac{\cos(\pi/4)}{\cos(\pi/4 + \delta\varphi/2)}$$

- Huge increase at low temperature due to low σ_s' and relatively high σ_s''.

Quality $Q_s = G/R_s$ *in local limit*

$$\frac{Q_s}{Q_n} = \left(\frac{|\sigma_s|}{|\sigma_n|}\right)^{1/2} \frac{\cos(\pi/4)}{\cos(\pi/4 + \delta\varphi/2)}$$

- Huge increase at low temperature due to low σ_s' and relatively high σ_s''.

- Absolute maxima at $T = 0K$, and $\gamma = 0$.
- Maximum for fixed $T \neq 0K$ at nonzero pair breaking.

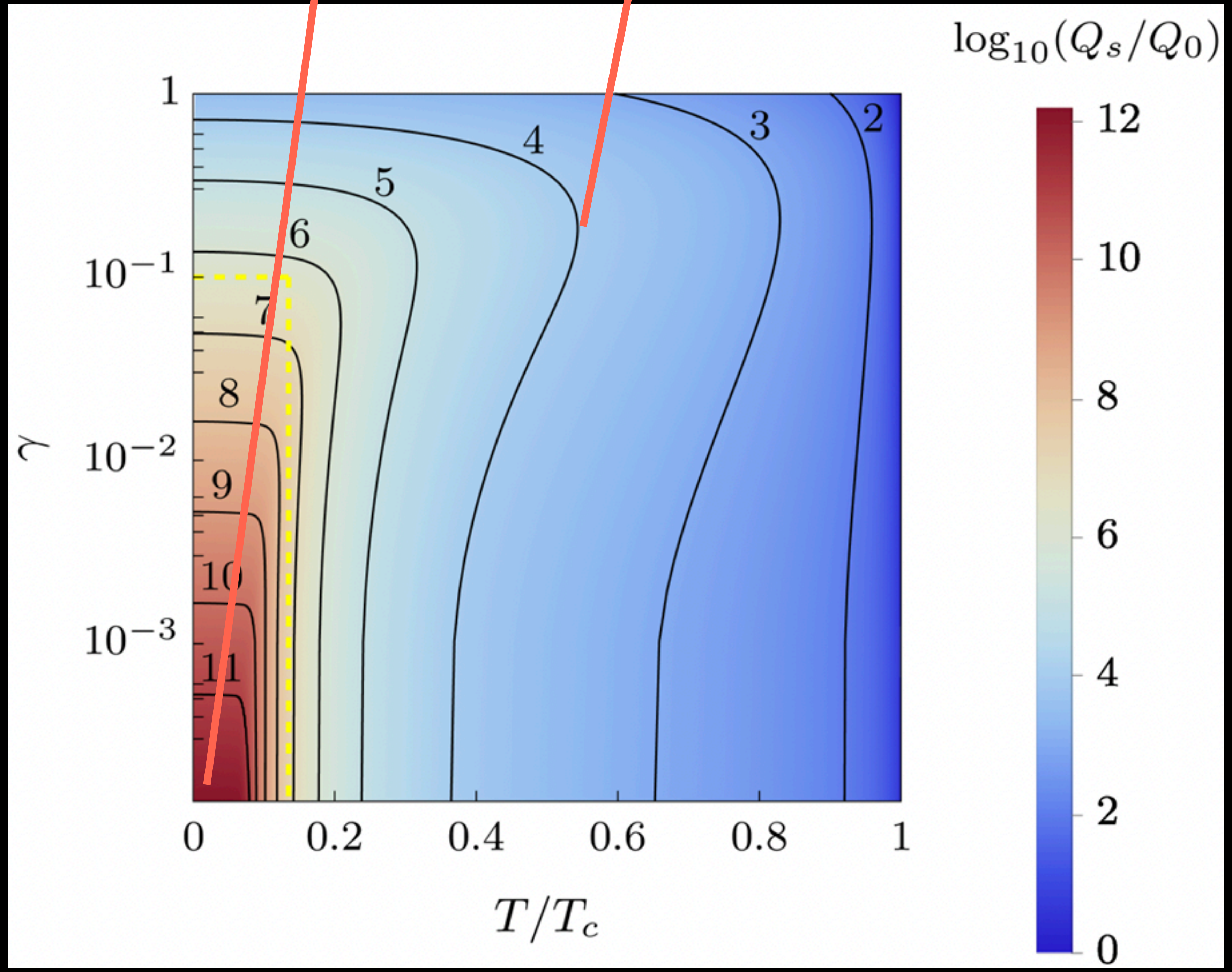

$\gamma_s \approx 0.13, \quad f = 1.3\,GHz, \quad \Delta_{00} = 2\,meV$

Quality $Q_s = G/R_s$ in local limit

$$\frac{Q_s}{Q_n} = \left(\frac{|\sigma_s|}{|\sigma_n|}\right)^{1/2} \frac{\cos(\pi/4)}{\cos(\pi/4 + \delta\varphi/2)}$$

- Huge increase at low temperature due to low σ_s' and relatively high σ_s''.

- Absolute maxima at $T = 0K$, and $\gamma = 0$.
- Maximum for fixed $T \neq 0K$ at nonzero pair breaking.

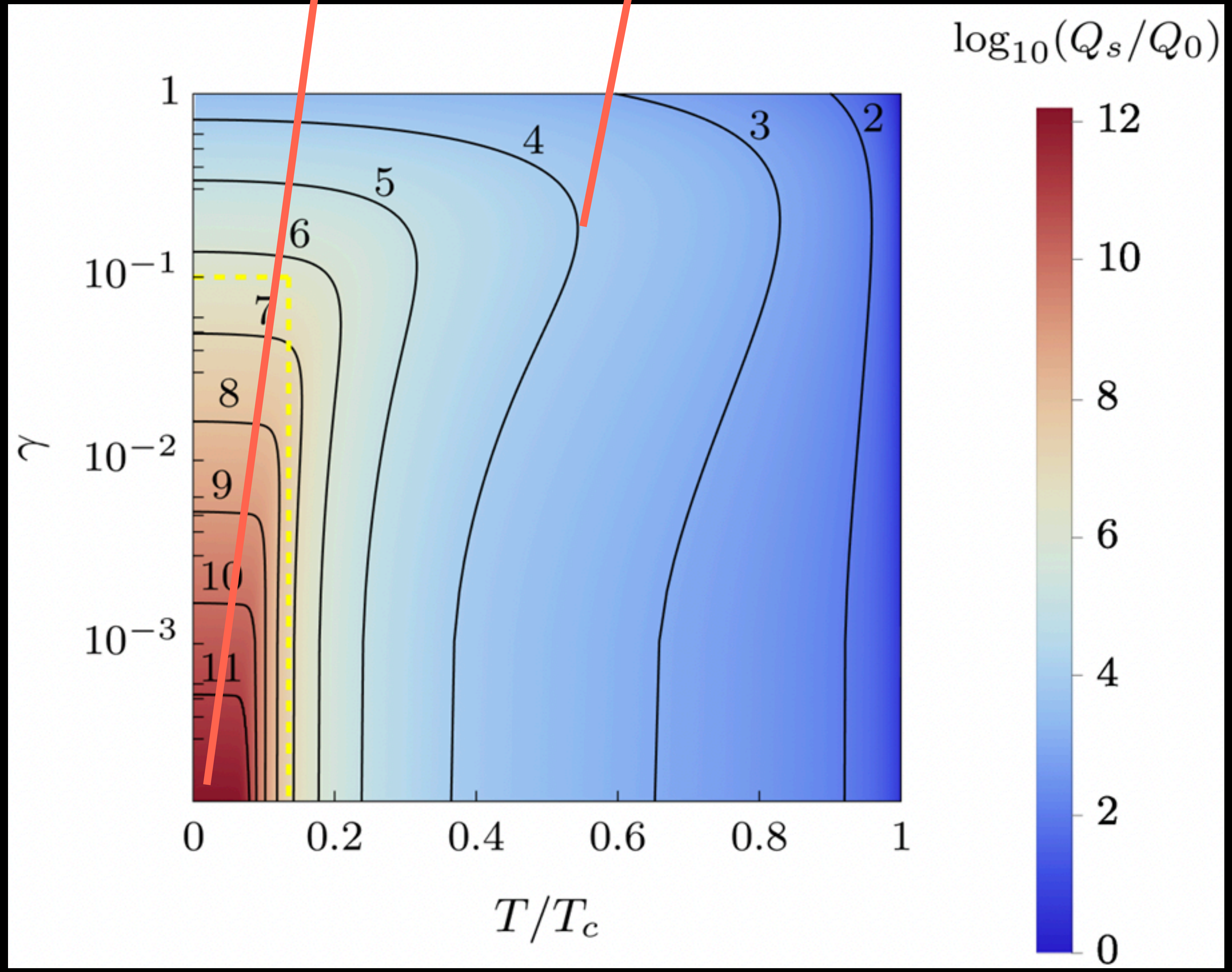

$\gamma_s \approx 0.13, \quad f = 1.3\, GHz, \quad \Delta_{00} = 2\, meV$

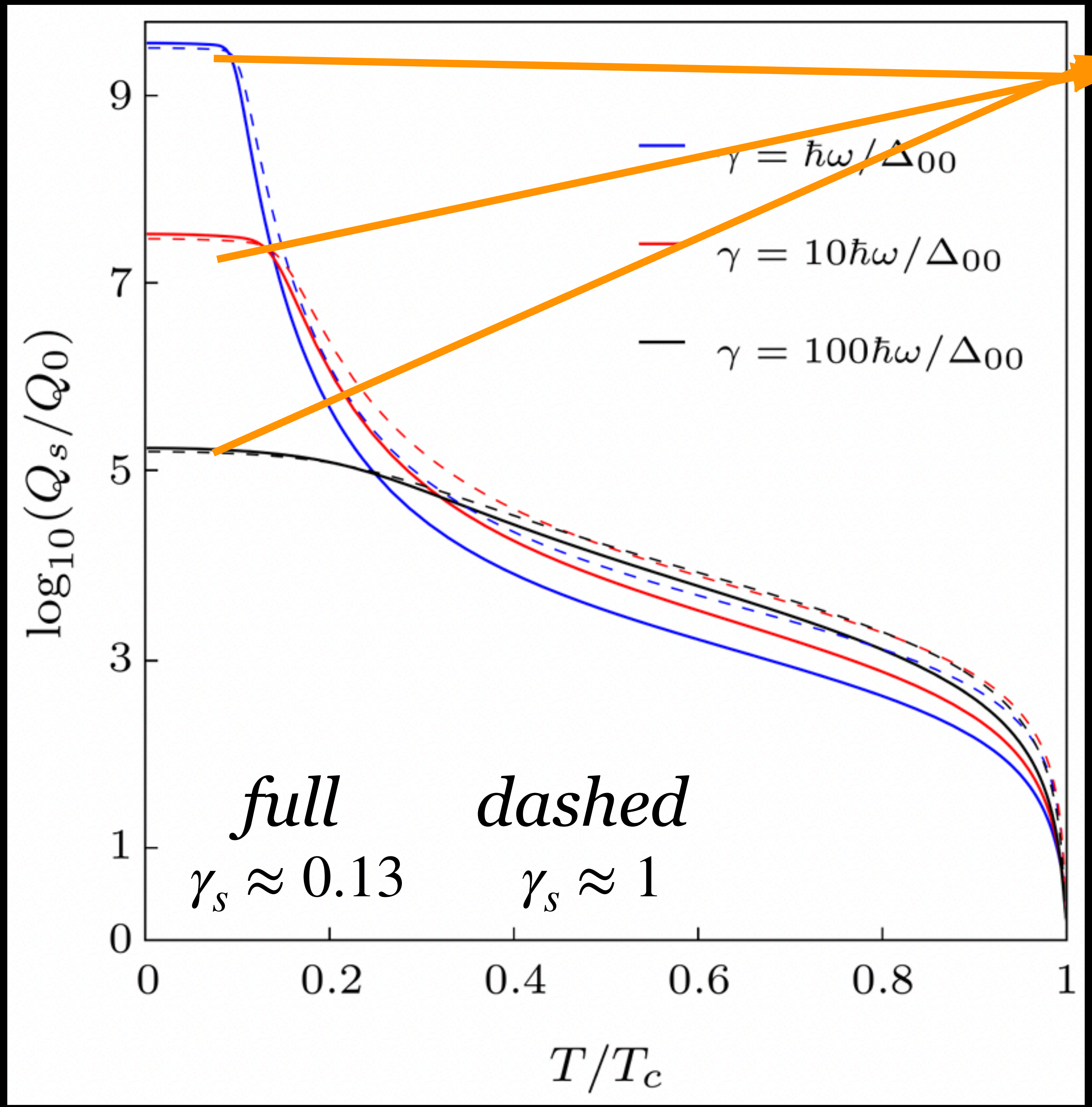

- High Quality "plateaus" for $T \lesssim T_p \approx 0.1 T_{c,0}$.
- Analysis showing the role of the in-gap states and Fermi-Dirac distribution can be found in arXiv:2409.04203
- Weakly dependent on $\gamma_s \lesssim 1$.

Surface (residual) resistance at $T = 0K$

$$\frac{R_s(0)}{R_n} = \sqrt{\frac{\sigma_0}{2}}\frac{\sigma_s'(0)}{\sigma_s''(0)^{3/2}}$$

Surface (residual) resistance at $T = 0K$

$$\frac{R_s(0)}{R_n} = \sqrt{\frac{\sigma_0}{2}} \frac{\sigma_s'(0)}{\sigma_s''(0)^{3/2}}$$

$$\frac{\sigma'(0)}{\sigma_0} = \frac{\gamma^2}{1+\gamma^2} \times \frac{\gamma_n}{\gamma_s + \sqrt{1+\gamma^2}}$$

- Pair-breaking subgap induced residual resistance.

$$\frac{\sigma''(0)}{\sigma_0} = \frac{2\Gamma_n}{\omega}\frac{n_s(0)}{n} = \frac{1}{2}\left(\frac{\delta}{\lambda_L(0)}\right)^2$$

- Ratio of the relevant penetration depths.

Surface (residual) resistance at $T = 0K$

$$\frac{R_s(0)}{R_n} = \sqrt{\frac{\sigma_0}{2}}\frac{\sigma_s'(0)}{\sigma_s''(0)^{3/2}} = \frac{2\sigma_s'(0)}{\sigma_0}\left(\frac{\lambda_L(0)}{\delta}\right)^3$$

$$\frac{\sigma'(0)}{\sigma_0} = \frac{\gamma^2}{1+\gamma^2} \times \frac{\gamma_n}{\gamma_s + \sqrt{1+\gamma^2}}$$

- Pair-breaking subgap induced residual resistance.

$$\frac{\sigma''(0)}{\sigma_0} = \frac{2\Gamma_n}{\omega}\frac{n_s(0)}{n} = \frac{1}{2}\left(\frac{\delta}{\lambda_L(0)}\right)^2$$

- Ratio of the relevant penetration depths.

Quality at $T = 0K$

$$\frac{Q_s(0)}{Q_n} = \frac{R_n}{R_s(0)} = \frac{4\sigma_0}{\sigma_s'(0)} \left(\frac{n_s(0)}{n} \frac{\Gamma_n}{\omega} \right)^{3/2}$$

- Role of superfluid fraction.

$$\frac{\sigma'(0)}{\sigma_0} = \frac{\gamma^2}{1+\gamma^2} \times \frac{\gamma_n}{\gamma_s + \sqrt{1+\gamma^2}}$$

- Pair-breaking subgap induced residual resistance.

Quality at $T = 0K$

$$\frac{Q_s(0)}{Q_n} = \frac{R_n}{R_s(0)} = \frac{4\sigma_0}{\sigma_s'(0)}\left(\frac{n_s(0)}{n}\frac{\Gamma_n}{\omega}\right)^{3/2}$$

- Role of superfluid fraction.

$$\frac{\sigma'(0)}{\sigma_0} = \frac{\gamma^2}{1+\gamma^2} \times \frac{\gamma_n}{\gamma_s + \sqrt{1+\gamma^2}}$$

- Pair-breaking subgap induced residual resistance.

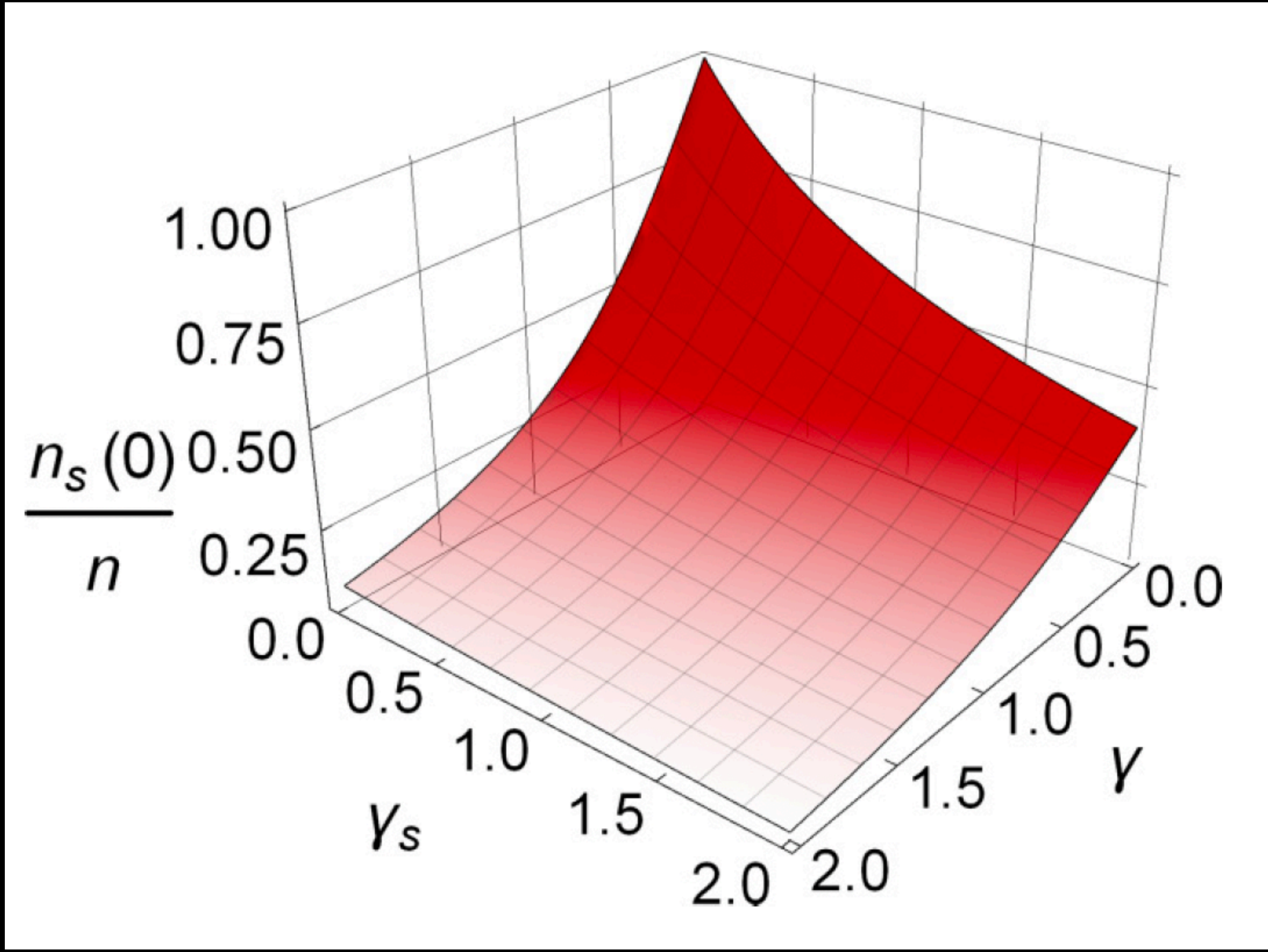

F. H. and R. Hlubina, Phys. Rev. B 96, 014509 (2017)

Quality at $T = 0K$

$$\frac{Q_s(0)}{Q_n} = \frac{R_n}{R_s(0)} = \frac{4\sigma_0}{\sigma_s'(0)}\left(\frac{n_s(0)}{n}\frac{\Gamma_n}{\omega}\right)^{3/2}$$

- Role of superfluid fraction.

$$\frac{\sigma'(0)}{\sigma_0} = \frac{\gamma^2}{1+\gamma^2} \times \frac{\gamma_n}{\gamma_s + \sqrt{1+\gamma^2}}$$

- Pair-breaking subgap induced residual resistance.

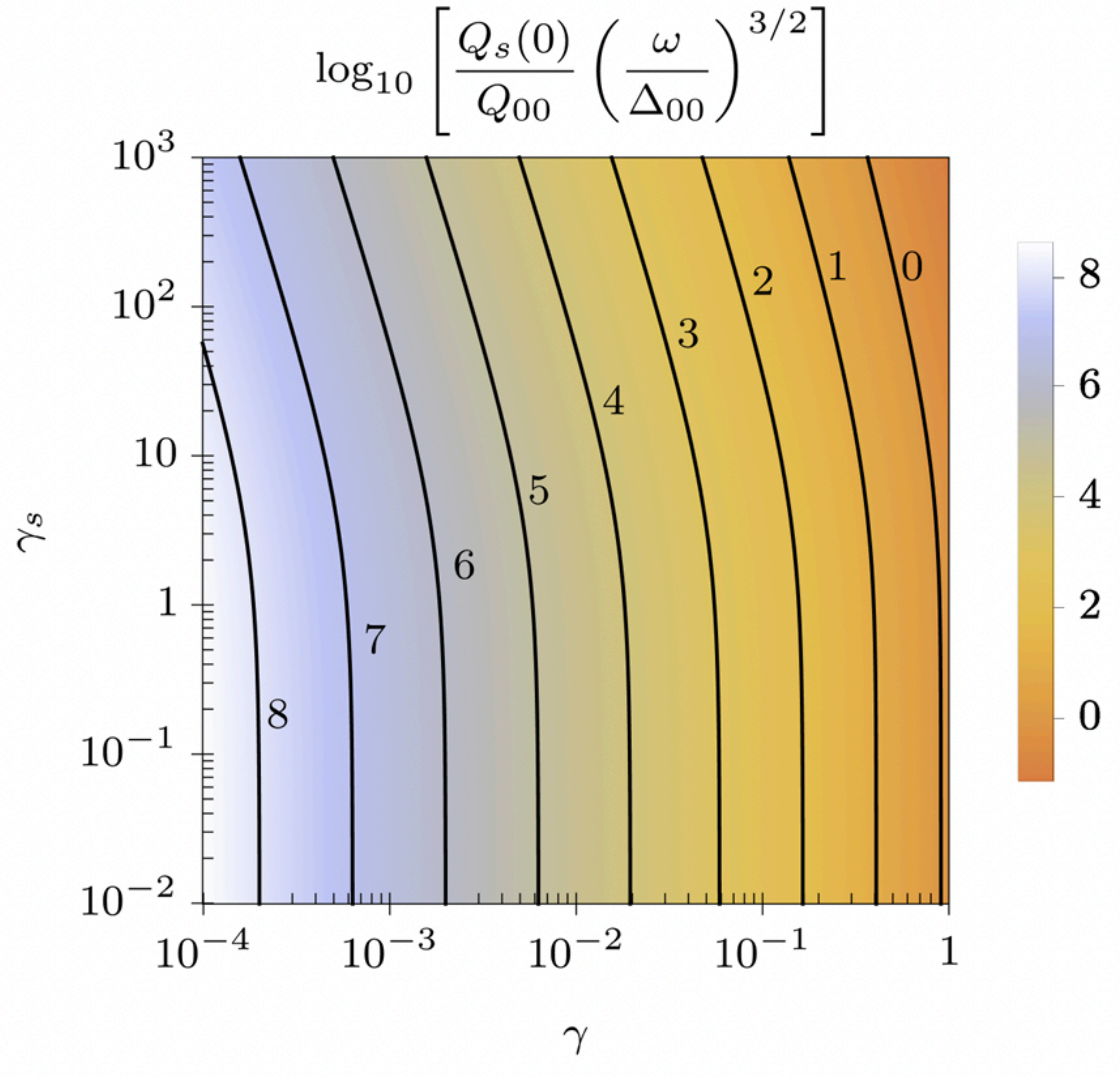

- The different roles of pair-breaking and pair-conserving scattering.
- Role of pair-conserving disorder changes.

Quality at $T = 0K$

Reduced scattering rates exercise

$$\frac{Q_s(0)}{Q_n} = \sqrt{\frac{2}{\sigma_0} \frac{\sigma_s''(0)^{3/2}}{\sigma_s'(0)}}$$

- Leading order of scattering rates

$$\sigma_s'(0)/\sigma_0 \approx \gamma^2(\gamma + \gamma_s) \qquad \sigma_s''(0)/\sigma_0 \approx 2(\Gamma + \Gamma_s)/\omega$$

$$\frac{Q_s(0)}{Q_n} = 4\left(\frac{\Delta_0}{\omega}\right)^{3/2} \frac{\sqrt{\gamma + \gamma_s}}{\gamma^2}$$

- Specific numbers

$$f = 1.3\text{GHz}$$

$$\gamma = \gamma_s \approx 2.7 \times 10^{-3}$$

$$\Delta_0 = 2\text{meV}$$

$$Q_s(0) \sim 10^8 Q_n$$

Focusing on Nb_3Sn

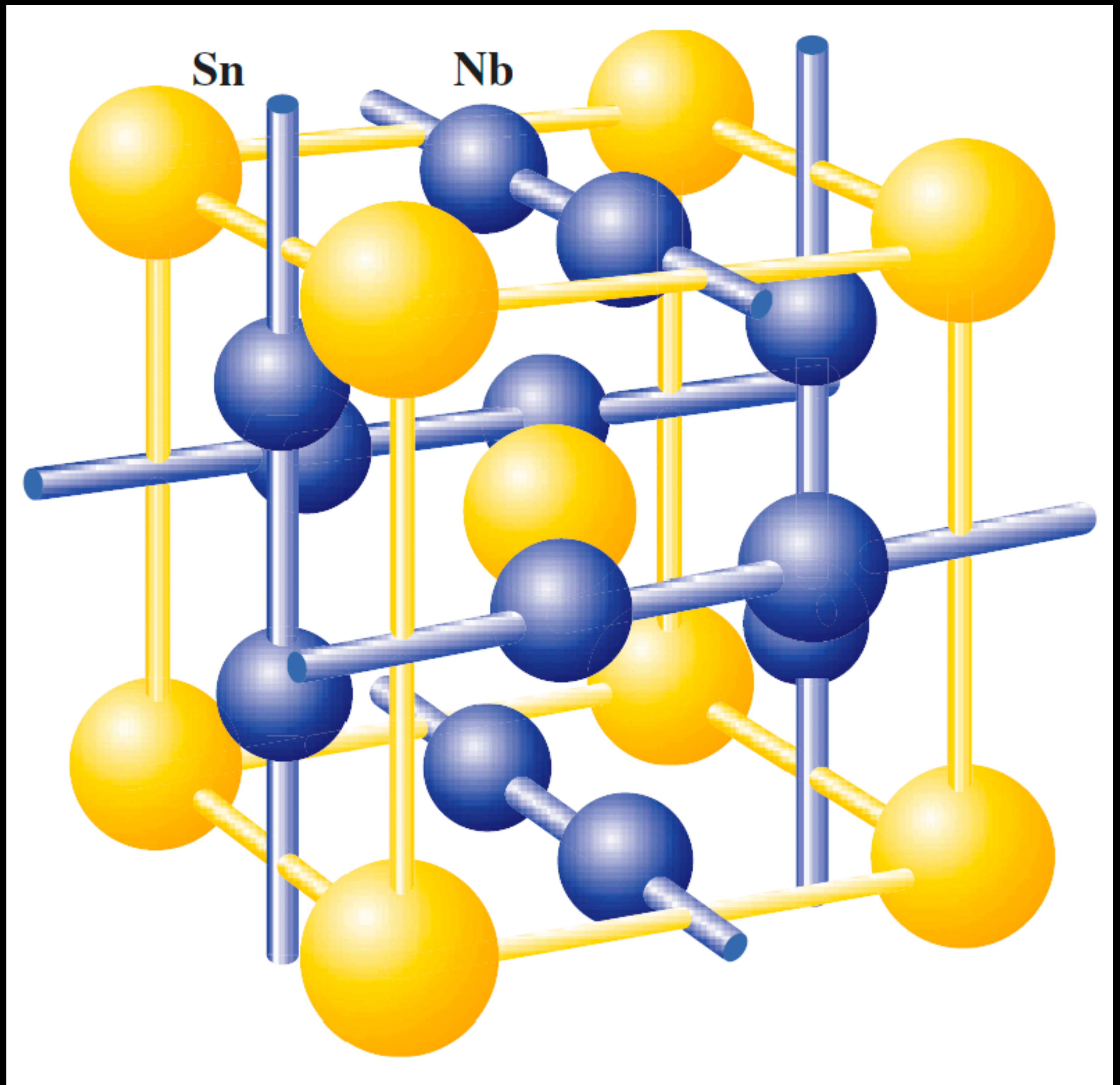

A15 Crystal structure of Nb_3Sn.

S. E. Posen, Understanding and overcoming limitations in Nb_3Sn superconducting RF cavities, PhD Thesis, Cornell University (2015), and references therein.

Focusing on Nb_3Sn

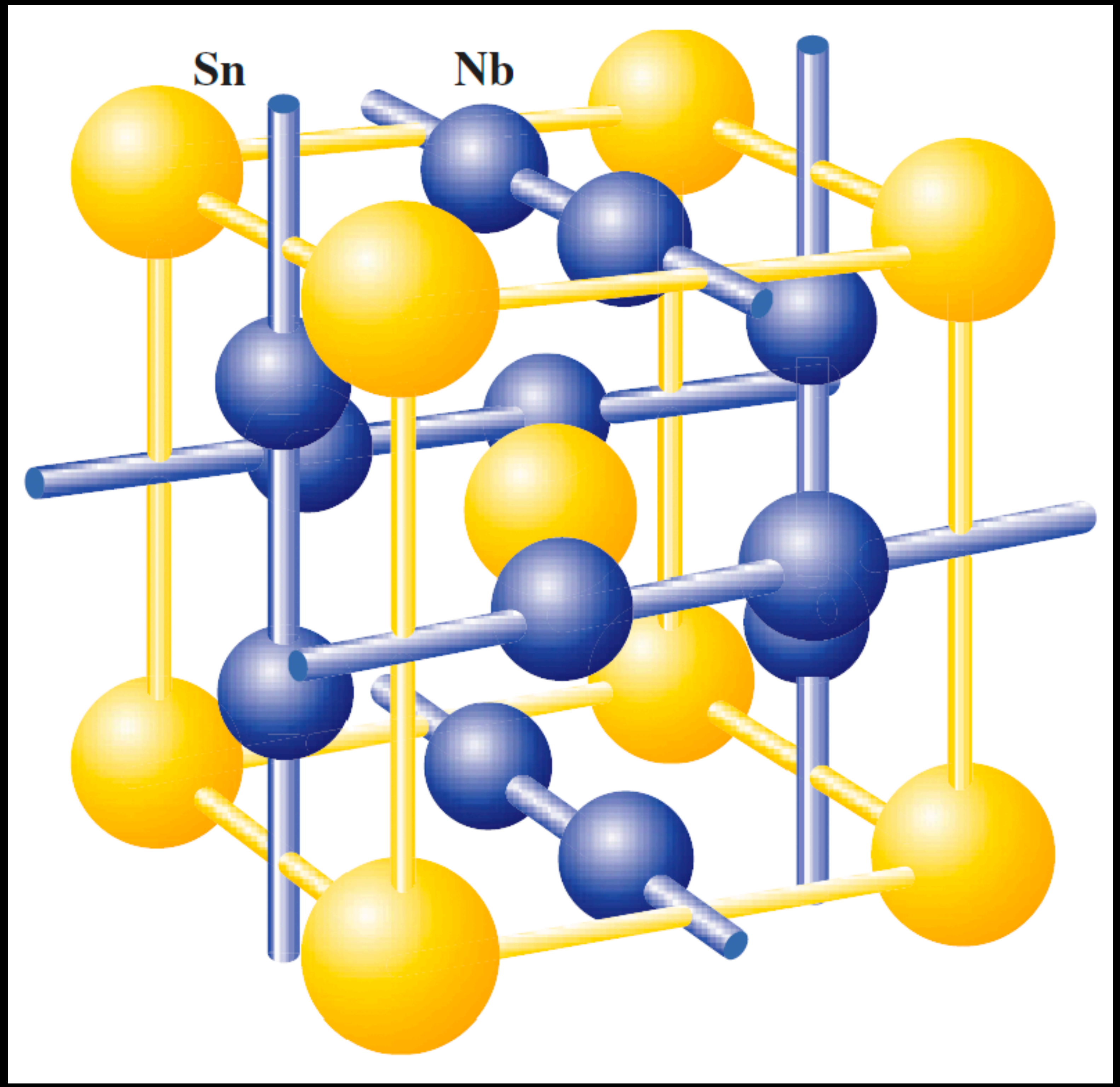

A15 Crystal structure of Nb_3Sn.

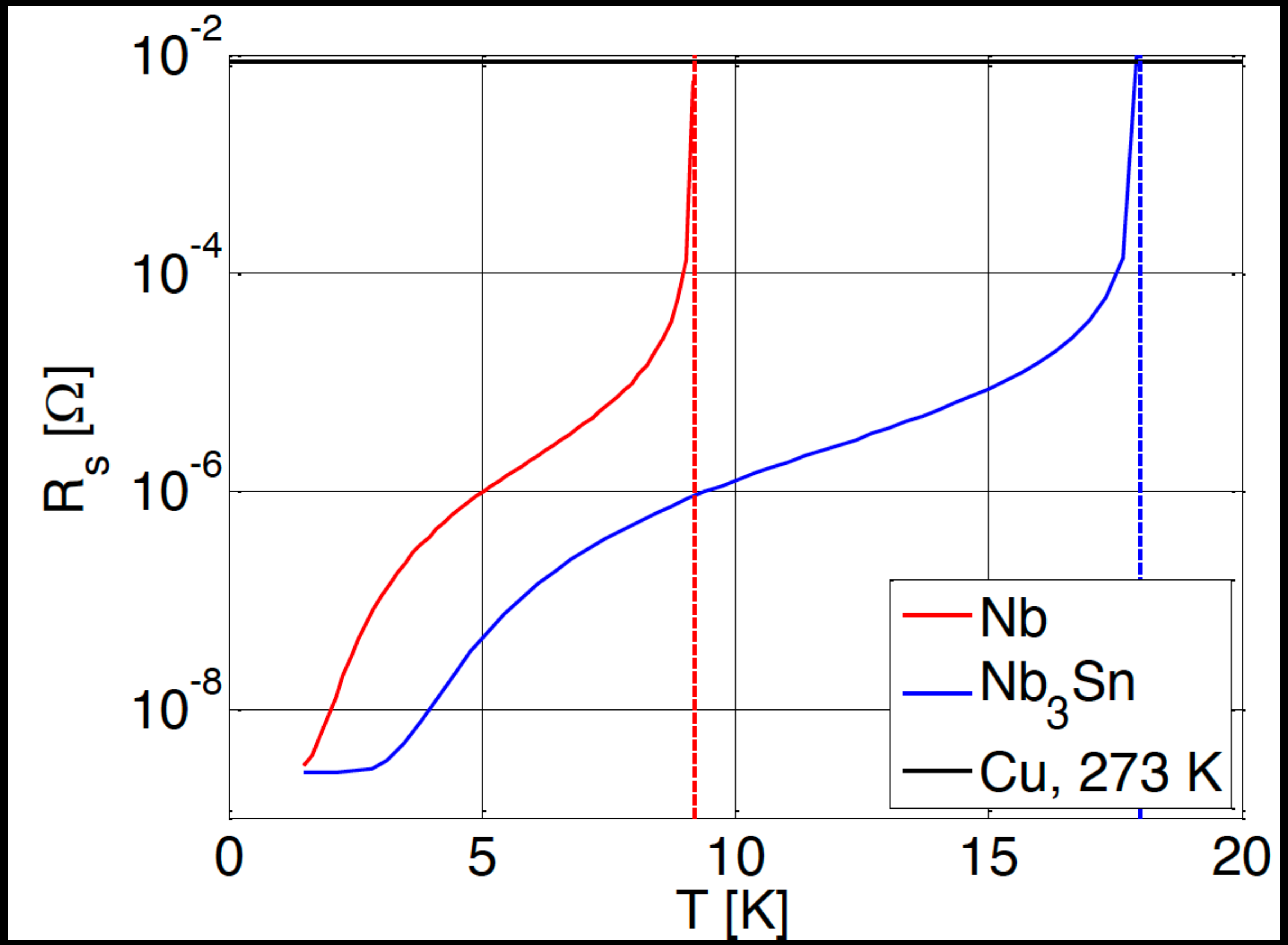

$\lambda_{L0} = 89\text{nm}$ $\ell = 4.8\text{nm}$ $\xi_0 = 7\text{nm}$

$\lambda_{L,0} \gg \ell$ $\gamma_n = \sqrt{2}\xi_0/\ell \approx 2$

$\Delta_0 \approx 3.5\text{meV}$

S. E. Posen, Understanding and overcoming limitations in Nb_3Sn superconducting RF cavities, PhD Thesis, Cornell University (2015), and references therein.

Ballpark estimate of $R_s(0)$ in case of Nb_3Sn

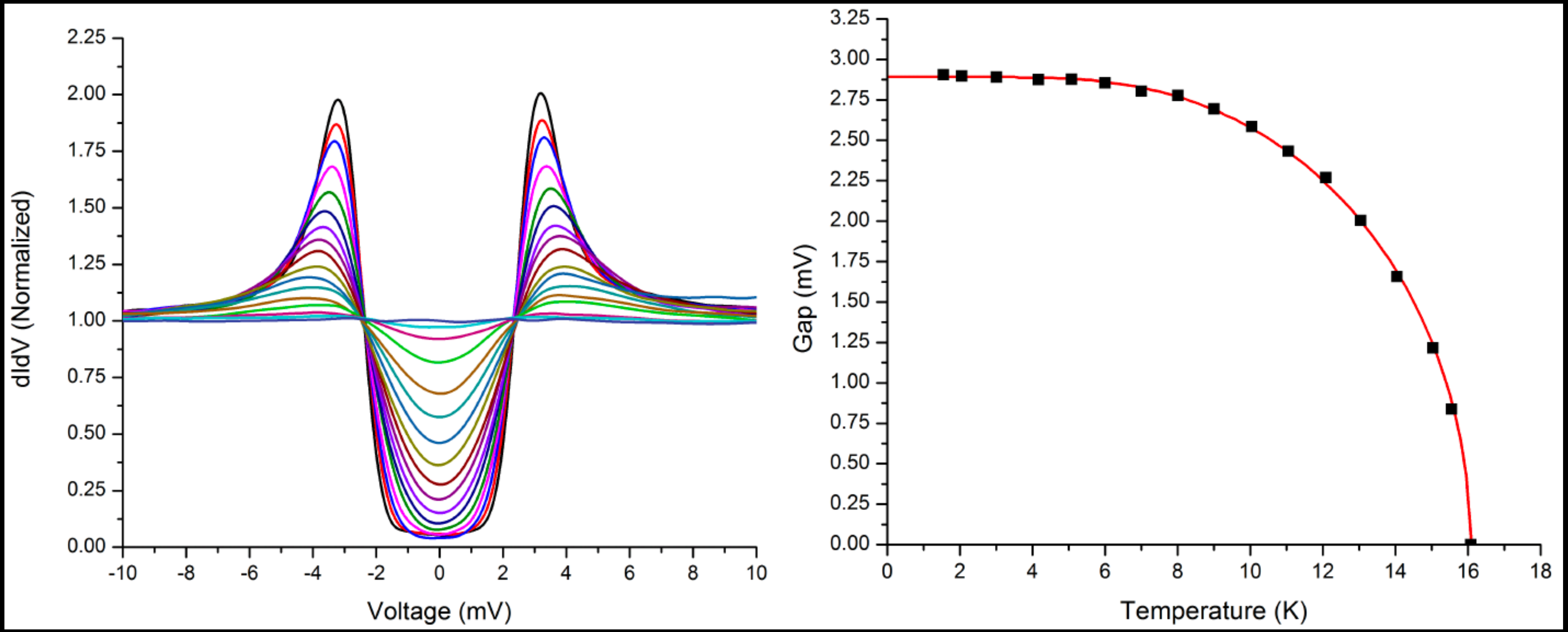

S. E. Posen, Understanding and overcoming limitations in Nb_3Sn superconducting RF cavities, PhD Thesis, Cornell University (2015), and references therein.

$$T_c = 17.9K \qquad T_{c,\max} \equiv T_{c,0} = 18.3K$$

$$\gamma \approx 2 \times 10^{-2}$$

Ballpark estimate of $R_s(0)$ in case of Nb_3Sn

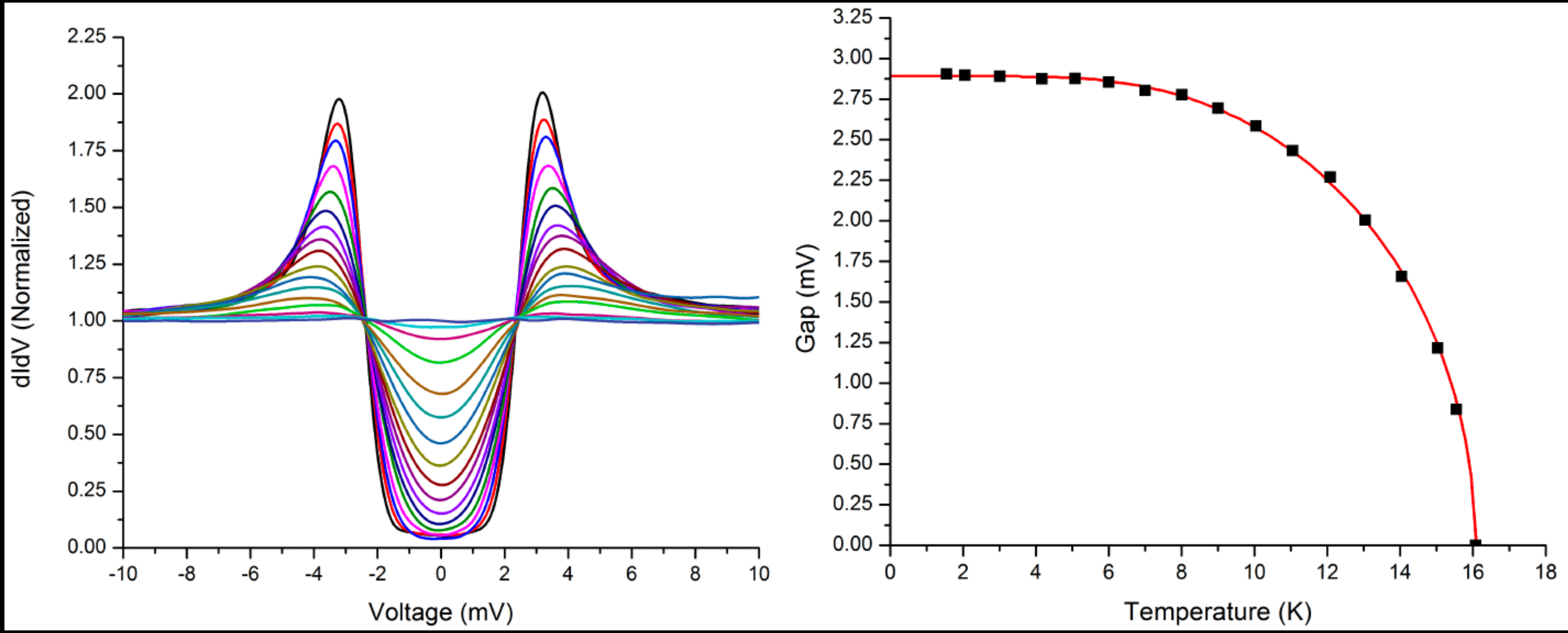

S. E. Posen, Understanding and overcoming limitations in Nb_3Sn superconducting RF cavities, PhD Thesis, Cornell University (2015), and references therein.

$\gamma \ll 1$ and $\gamma_s \sim 1$ and $\hbar\omega \sim \mu\mathrm{eV}$

$$R_s(0) = \frac{\mu_0 \hbar \lambda_{L0} (\omega\gamma)^2}{4\Delta_0(1+\gamma_s)} \left(\frac{n}{n_s(0)} \right)^{3/2} \approx 0.2\mathrm{n}\Omega$$

Experimental value: $R_{\mathrm{res}} \approx 8.5\mathrm{n}\Omega$

$T_{\mathrm{c}} = 17.9K \quad T_{\mathrm{c,\,max}} \equiv T_{\mathrm{c},0} = 18.3K$

$\gamma \approx 2 \times 10^{-2}$

Ballpark estimate of $R_s(0)$ in case of Nb_3Sn

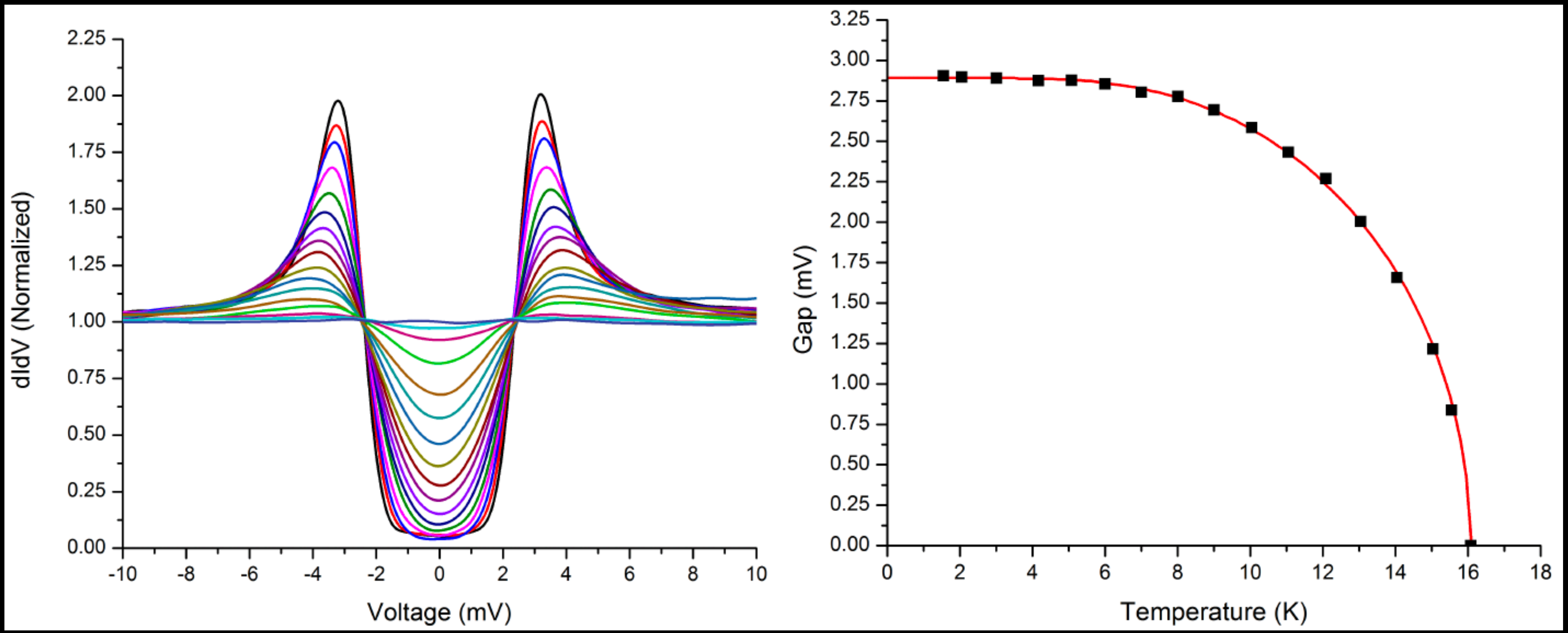

S. E. Posen, Understanding and overcoming limitations in Nb_3Sn superconducting RF cavities, PhD Thesis, Cornell University (2015), and references therein.

$\gamma \ll 1$ and $\gamma_s \sim 1$ and $\hbar\omega \sim \mu\text{eV}$

$$R_s(0) = \frac{\mu_0 \hbar \lambda_{L0} (\omega\gamma)^2}{4\Delta_0(1+\gamma_s)} \left(\frac{n}{n_s(0)}\right)^{3/2} \approx 0.2\text{n}\Omega$$

Experimental value: $R_{\text{res}} \approx 8.5\text{n}\Omega$

$$T_{\text{c}} = 17.9K \qquad T_{\text{c, max}} \equiv T_{\text{c},0} = 18.3K$$

$$\gamma \approx 2 \times 10^{-2}$$

Discrepancy reasons

- Ignored anisotropy of the gap -> Oversimplified model
- Ignoring Two Level Systems... -> Only pair breaking scattering contribution

Summary & Conclusions I.

Frequency Shift

- Despite omitting the inhomogeneity effects, DS framework provides qualitatively (and quantitatively) reasonable results with the same numerical complexity as the Mattis-Bardeen theory.

- Various frequency shift regimes (Foot, Bump, Dip & Bump and Dip) assuming low disorder can be systemically identified.

- Addressing the moderately clean regime, we describe the frequency shift slope $\delta f'(\Theta) = \partial\delta f(\Theta)/\partial\Theta|_{\Theta=0}$ with the simple function of pair-conserving and pair-breaking scattering rates.

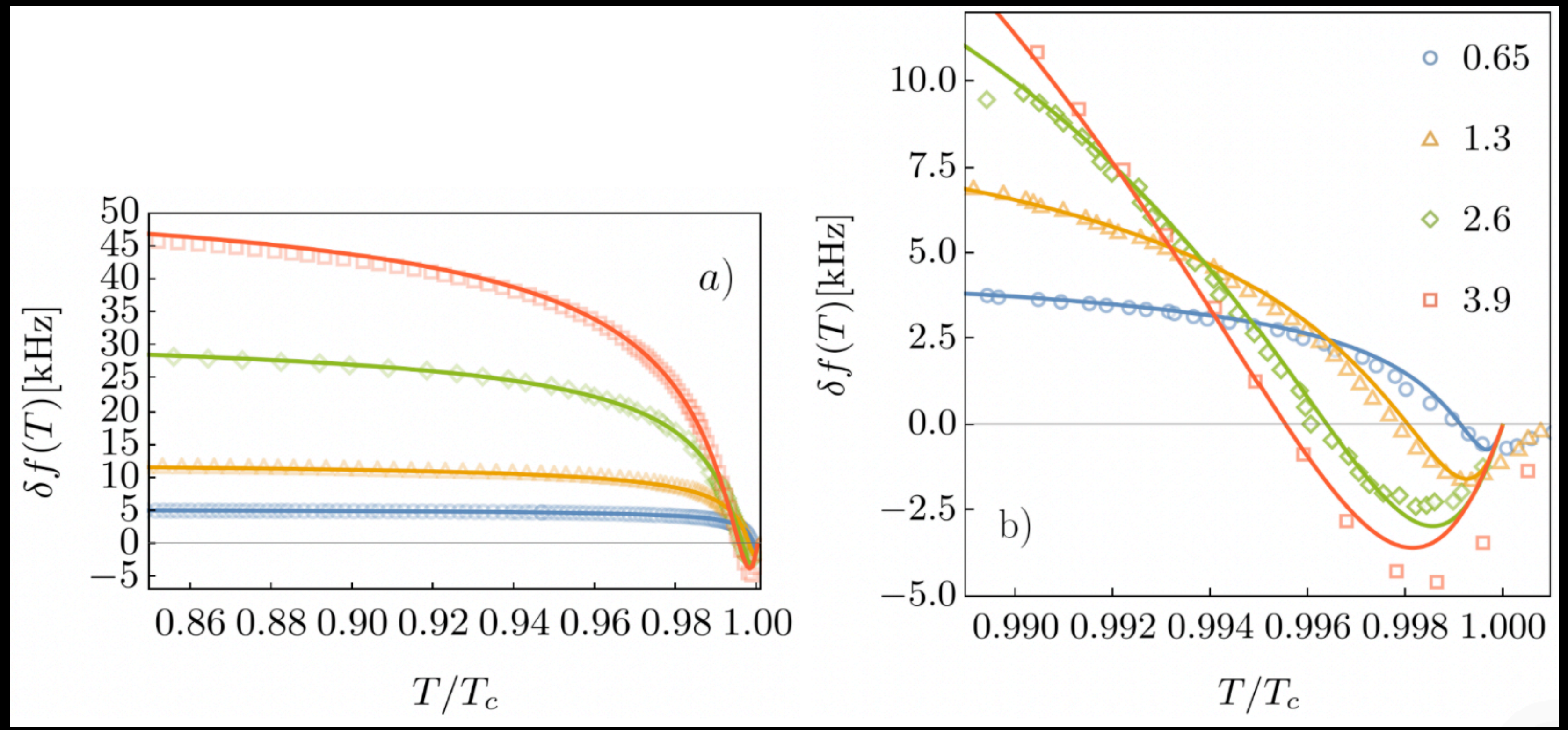

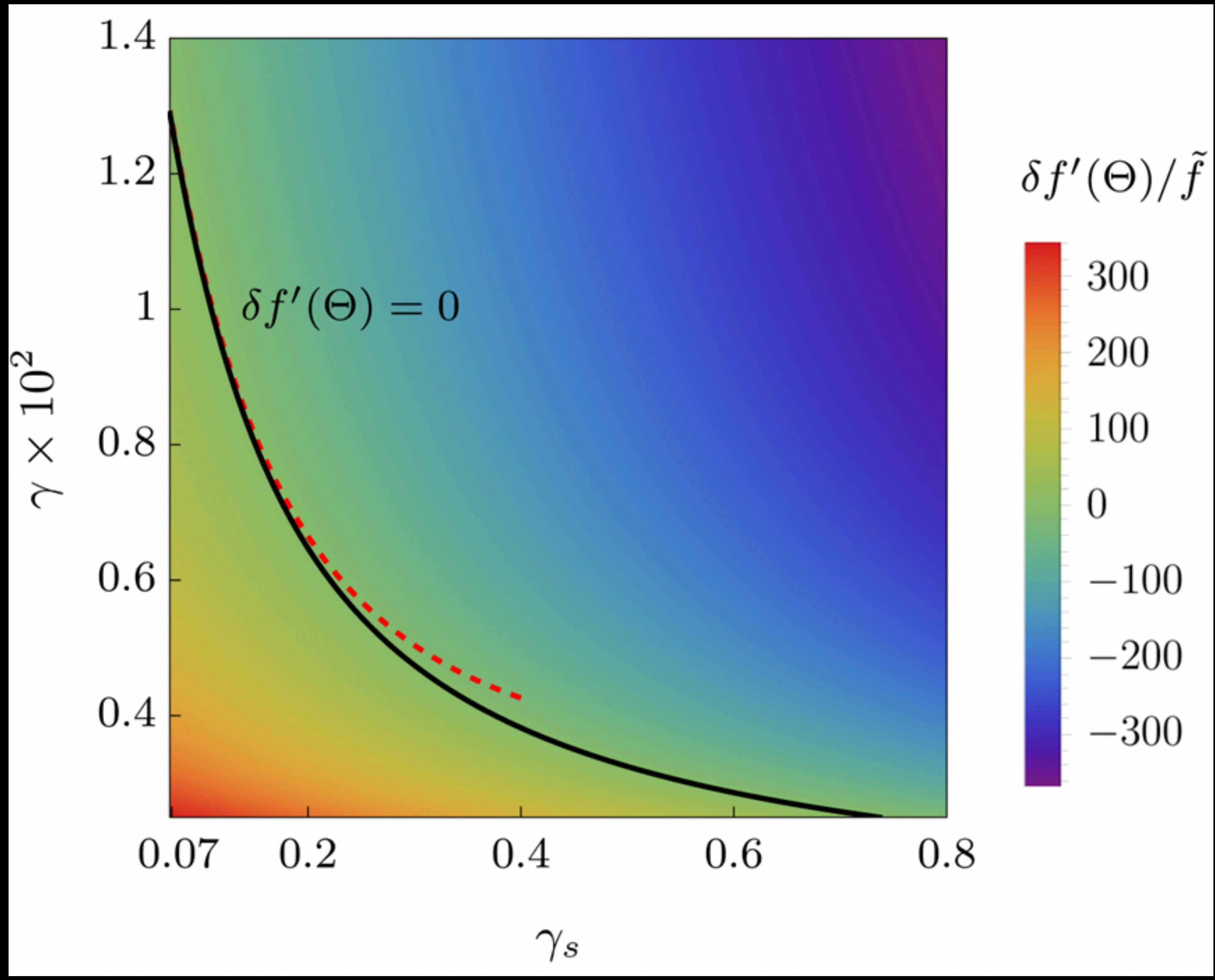

Summary & Conclusions II.

Quality

- Analysis of the high quality plateaus at low temperature and low disorder.

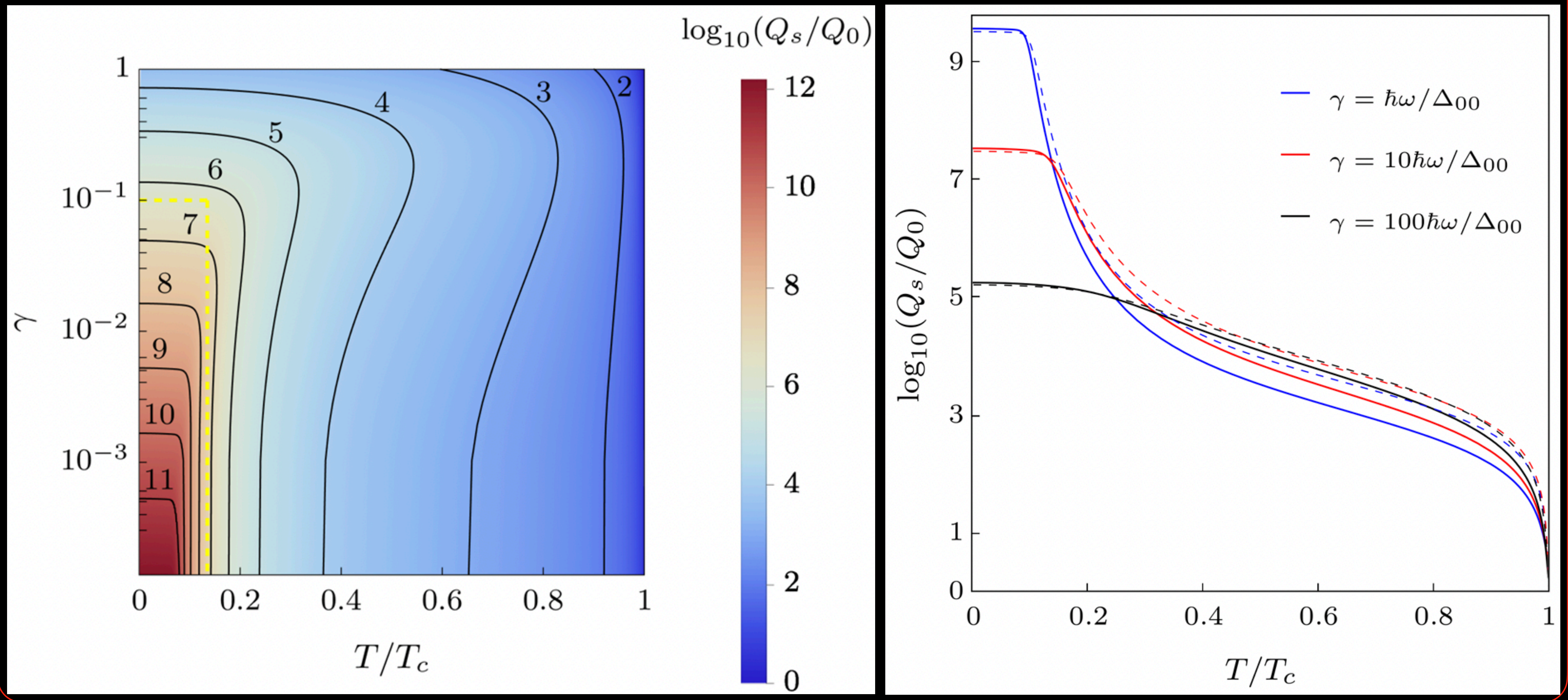

- Analysis of the quality factor at zero Kelvin Temperature shows different influence of pair-breaking and pair-conserving disorder.

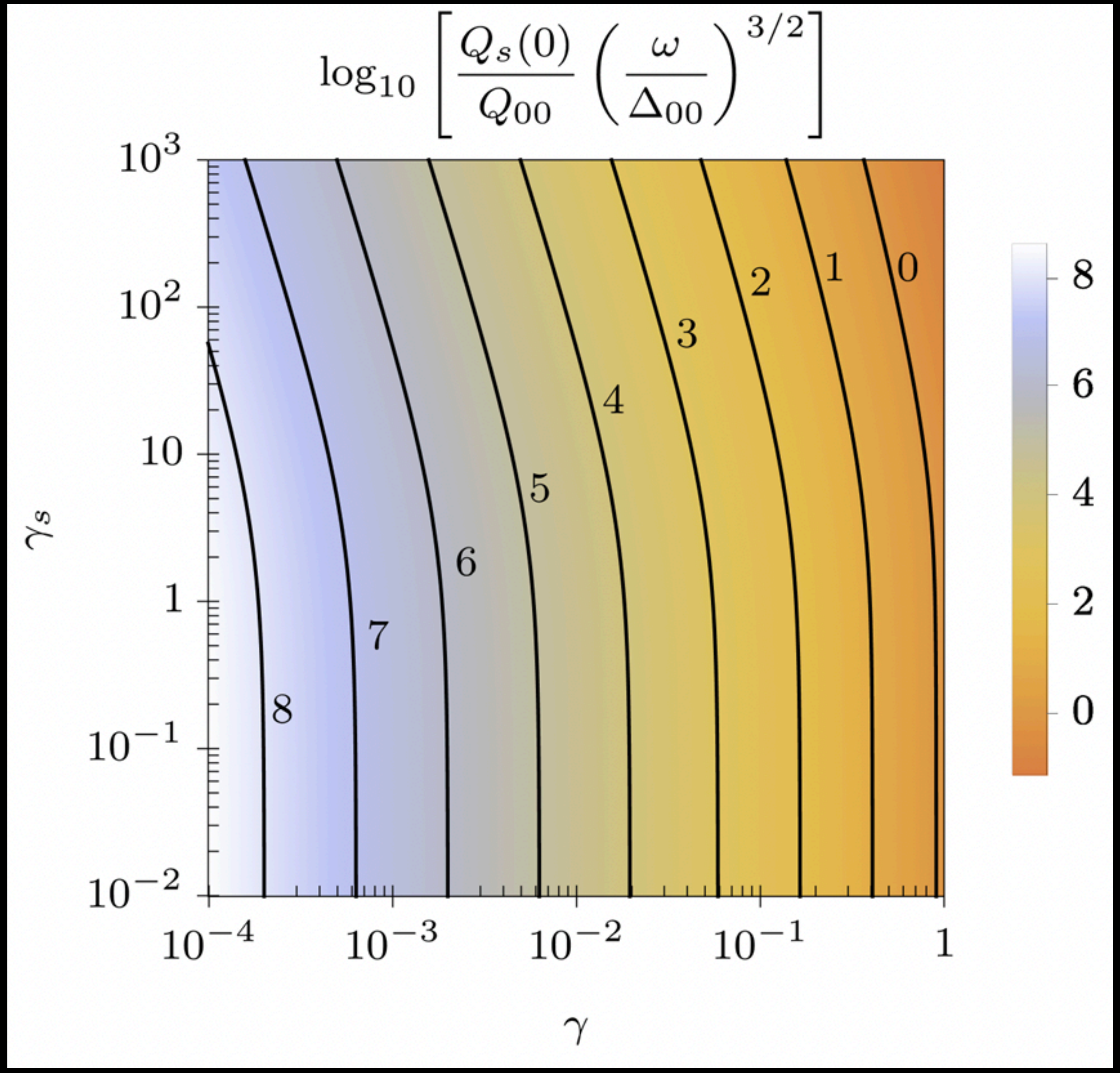

- *For further details: arXiv:2409.04203*

Summary & Conclusions II.

Quality

- Analysis of the high quality plateaus at low temperature and low disorder.

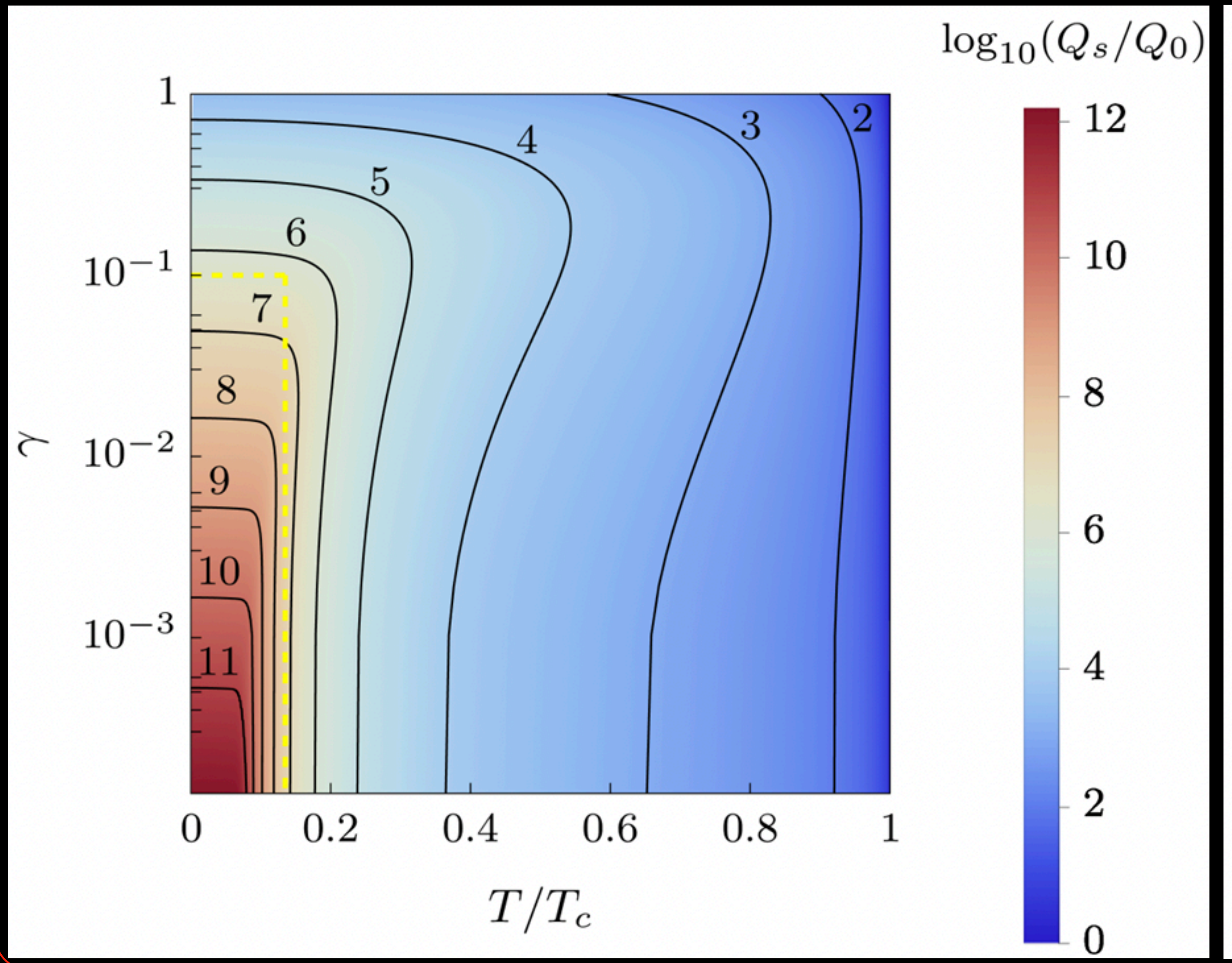

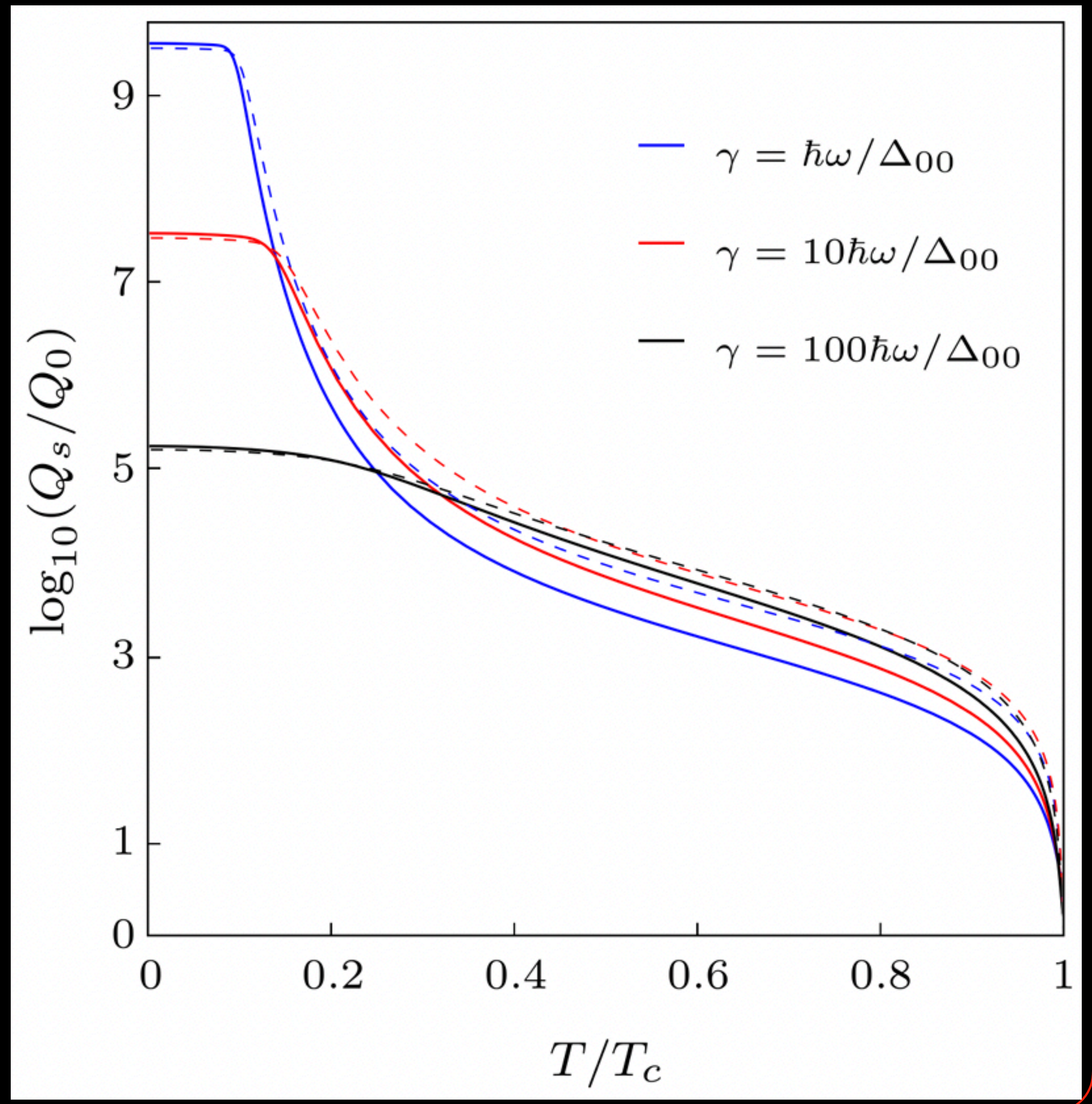

- Analysis of the quality factor at zero Kelvin Temperature shows different influence of pair-breaking and pair-conserving disorder.

- *For further details: arXiv:2409.04203*

Coherent Potential Approximation